J. Fluid Mech. (1993), *vol.* 255, *pp.* 565–595

Sedimentation of particles in polymer solutions

By YAOQI JOE LIU AND DANIEL D. JOSEPH

Department of Aerospace Engineering and Mechanics, University of Minnesota, 107 Akerman Hall, 110 Union Street SE, Minneapolis, MN 55455, USA

(Received 29 June 1992 and in revised form 28 April 1993)

In this paper, we present detailed and systematic experimental results on the sedimentation of solid particles in aqueous solutions of polyox and polyacrylamide, and in solutions of polyox in glycerin and water. The tilt angles of long cylinders and flat plates falling in these viscoelastic liquids were measured. The effects of particle length, particle weight, particle shape, liquid properties and liquid temperature were determined. In some experiments, the cylinders fall under gravity in a bed with closely spaced walls. No matter how or where a cylinder is released the axis of the cylinder centres itself between the close walls and falls steadily at a fixed angle of tilt with the horizontal. A discussion of tilt angle may be framed in terms of competition between viscous effects, viscoelastic effects and inertia. When inertia is small, viscoelasticity dominates and the particles settle with their broadside parallel or nearly parallel to the direction of fall. Normal stresses acting at the corners of rectangular plates and squared-off cylinders with flat ends cause shape tilting from the vertical. Cylinders with round ends and cone ends tilt much less in the regime of slow flow. Shape tilting is smaller and is caused by a different mechanism to tilting due to inertia. When inertia is large the particles settle with their broadside perpendicular to the direction of fall. The tilt angle varies continuously from 90° when viscoelasticity dominates to 0° when inertia dominates. The balance between inertia and viscoelasticity was controlled by systematic variation of the weight of the particles and the composition and temperature of the solution. Particles will turn broadside-on when the inertia forces are larger than viscous and viscoelastic forces. This orientation occurred when the Reynolds number Re was greater than some number not much greater than one in any case, and less than 0.1 in Newtonian liquids and very dilute solutions. In principle, a long particle will eventually turn its broadside perpendicular to the stream in a Newtonian liquid for any $Re > 0$, but in a viscoelastic liquid this turning cannot occur unless $Re > 1$. Another condition for inertial tilting is that the elastic length λU should be longer than the viscous length ν/U where U is the terminal velocity, ν is the kinematic viscosity and $\lambda = \nu/c^2$ is a relaxation time where c is the shear wave speed measured with the shear wave speed meter (Joseph 1990). The condition $M = U/c > 1$ is provisionally interpreted as a hyperbolic transition of solutions of the vorticity equation analogous to transonic flow. Strong departure of the tilt angle from $\theta = 90°$ begins at about $M = 1$ and ends with $\theta = 0°$ when $1 < M < 4$.

1. Introduction

Michele, Pätzold & Donis (1977) showed that chains of small spheres (~ 70 μm) may be created and aligned in the direction of shearing between parallel plates. Less compelling observations of the same phenomena were reported earlier by Highgate (1966) and by Highgate & Whorlow (1969). Petit & Noetinger (1988) found that small spheres (~ 40 μm) sheared by a rectilinear 200 Hz oscillation of parallel plates

align in the direction of shear when the liquid is viscoelastic and across the direction of shear when the liquid is Newtonian.

In a different kind of experiment involving steady flow without shear, Joseph *et al.* (1992*b*) showed that large spheres, several millimetres in diameter, sedimenting in a fluid filled channel will arrange themselves so that the line of centres between neighbouring spheres is across the stream in a viscous liquid and parallel to the stream in a viscoelastic liquid when the fall velocity is small but across the stream again when the fall velocity is large. They noted that the flow induced anisotropy of sedimenting spherical particles is associated with the natural orientation of long bodies, longside along the stream when viscoelasticity dominates and perpendicular to the stream when inertia dominates. The present paper focuses on the orientation effects on long bodies.

It is well known that the orientation of sedimenting long bodies in Stokes flow is undetermined; there are no hydrodynamic couples to turn a long body in steady flow. Slow flows of Newtonian liquids reduce to Stokes flow asymptotically, but at a finite Reynolds number, no matter how small, inertia will eventually have its way and turn the broadside of a long body perpendicular to the stream (Cox 1965). It is also known that flows of different viscoelastic fluids reduce to Stokes flow when the flows are sufficiently slow and slowly varying. Turning couples appear at second order.

Leal (1975) has studied the sedimentation of slender bodies in a second-order fluid with inertia neglected. He considers only those non-Newtonian effects resulting from the disturbance velocity field generated by the lowest-order geometry independent approximation of the Stokeslet distribution used in slender-body theory. He finds that freely translating particles with fore–aft symmetry exhibit a single stable orientation with axis of revolution vertical.

Brunn (1977) worked on asymptotic theory in powers of the Weissenberg number with inertia neglected and found that to leading order a transversally isotropic particle will change its orientation until it becomes either parallel or perpendicular to the direction of the external force. His work and other works about the slow motions of particles in non-Newtonian fluids with inertia neglected were reviewed by Leal (1980). The mechanism which aligns a slender body with the stream is not easy to extract from these perturbation analyses.

In the appendix of Leal's (1975) paper, Leal & Zana reported preliminary experimental observations of the motion of slender cylinders (~ 0.7 inches long with aspect ratios of 28 and 66) falling in glycerin and also a 0.5% aqueous solution of polyacrylamide (AP-30). The orientation of this cylinder in glycerin was said to be determined by the initial orientation but the same long body rotated into a vertical orientation in the AP-30 solution regardless of the initial orientation. Leal concluded that the viscoelastic properties of the fluid were responsible for the vertical orientation.

Chiba, Song & Horikawa (1986) studied the motion of slender cylinders (diameter = 0.612 mm, length = 30 mm and 60 mm) falling in water and in aqueous solutions of polyacrylamide and hydroxyethyl cellulose. They demonstrated that a slender body falling in a Newtonian liquid rotates to adopt a horizontal orientation, whereas in viscoelastic liquids it rotates toward a vertical orientation. For less concentrated solutions the body is not able to reach the vertical orientation and also moves sideways with a constant angle of tilt. The time-dependent orientation of the thin cylinder was studied at different concentrations and related to the shear thinning characteristics of the solution. They also considered the effect of variations of elasticity, supposing these to be associated with increasing concentration of polymer, but without reporting measurements of any viscoelastic parameters. They concluded that the angle that the axis of the cylinder makes with the vertical decreases with shear thinning and elasticity.

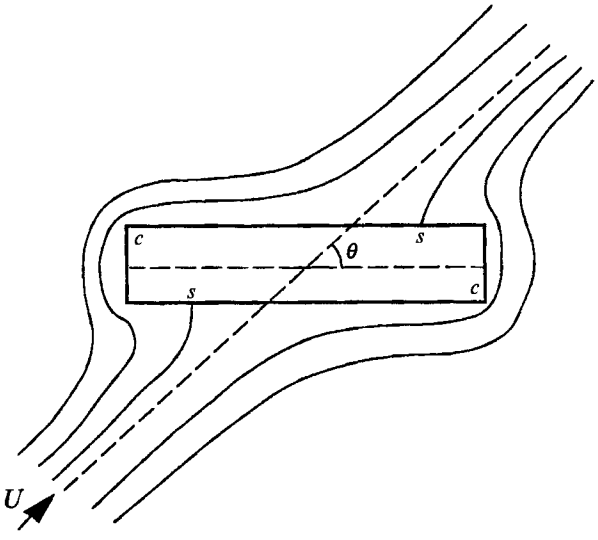

FIGURE 1. Potential flow past a cylinder. The pressure at stagnation points s will turn the broadside of the body into stream. If the extensional stress at s were reversed, as may be possible in a viscoelastic liquid, the body would line up with the stream. The same type of turning with the broadside parallel to the stream could be provided by normal stresses caused by strong shears at the corners c. In practice, viscosity will lead to boundary layers and wakes whose effects are not yet understood.

Cho, Cho & Park (1992) studied sedimentation of thin cylinders in aqueous solutions of polyacrylamide. Their cylinders were of the order of 1 mm with aspect ratios ranging from 10 to 100. The final orientation of the thin cylinder in the polyacrylamide solution was vertical, regardless of the initial launching orientation if the concentration was greater than 200 p.p.m. In contrast, the thin cylinder falls horizontally both in glycerin and in the Carbopol solution, regardless of the initial launching orientation of the cylinder. The tilt angle between the falling cylinder and the vertical axis parallel to gravity was measured for different concentrations and varied continuously from 90° in pure glycerin to 0° for concentrations greater than 200 p.p.m.

The work of Leal (1975) and Brunn (1977) shows also that shear thinning cannot be the only mechanism that causes a long body to fall with its axis vertical. They get this turning from a perturbation analysis in which shear thinning is not present. We see nose down turning in STP which is a constant viscosity (Boger) viscoelastic fluid. However, shear thinning combined with a fading memory of the places thinned may be important.

The coupled effects of inertia and viscoelasticity were not considered in the papers of Leal (1975, 1980), Brunn (1977), Chiba *et al.* (1986) or Cho *et al.* (1992), but the effects of inertia cannot be neglected in a general discussion of the orientation of sedimenting long bodies (see Joseph *et al.* 1992*b*).

The streamwise orientation of a long body is unstable in a viscous liquid, and it will always turn its broadside to the stream. An explanation (Thompson & Tait 1879) for this can be found in the couples which are produced by high pressures at the stagnation points on the long body shown in figure 1. The potential flow mechanism for turning long bodies broadside-on cannot provide the whole explanation at finite Reynolds numbers. In practice, wakes and skin friction enter into the description. Stokes flows around transversally isotropic bodies like cylinders and ellipsoids of revolution which have fore and aft symmetry are symmetric in the sense that the sum of moments of

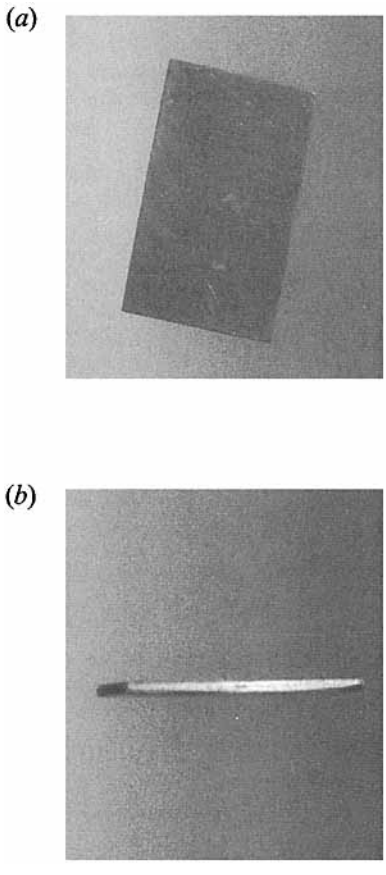

FIGURE 2. Photographs of flat plates falling in 2% aqueous polyacrylamide. (*a*) The aluminium plate settles slowly with its broadside parallel to gravity. (*b*) Steel plates are heavier and fall faster with their broadsides perpendicular to gravity.

traction vectors on the boundary of the body vanish. Inertia destroys this symmetry and generates a net turning couple which turns the broadside of the body into the stream. Inertia leads to strong moments when viscosity is neglected and viscosity leads to zero net moment when inertia is neglected. So we are led to believe that the turning couples arising from the inertially dominated potential flow mechanism operate also at finite Reynolds numbers.

The experiments of Joseph *et al.* (1992*b*) and especially the ones reported here show that the tilt transition is a phenomenon generated by the competition of viscoelasticity and inertia. We may consider the dependence of the orientation angle on the weight of the cylinder of fixed size and shape but different composition falling under gravity in one certain polymeric liquid of given composition and temperature in a fixed tank. If the light cylinder falls straight down, heavier cylinders will tilt and yet heavier cylinders will turn their broadside into the stream as they always do in a viscous fluid. This effect is especially dramatic in the sedimentation of flat plates (see figure 2).

The questions which are posed by this competition between inertia and viscoelasticity are: what are the dominant mechanisms controlling tilt and what dimensionless parameters are relevant? In viscous fluids only the Reynolds number, the ratio of inertial to viscous forces enters and inertia always wins. The body will always turn to

its broadside to the stream eventually no matter how small the Reynolds number. In the case of a viscoelastic fluid other physics and other parameters must enter since the body will never turn its broadside to the stream at small Reynolds numbers.

It did not at first occur to us that the change of orientation of long bodies sedimenting in different polymeric liquids could be framed as a change of type with features resembling those already seen in studies of delayed die swell (see Joseph 1990 (hereinafter referred to as J1990) and Joseph & Christodoulou 1993). The cylinders settle vertically, more or less, when the viscoelastic Mach number is less than some number not too much greater than one. When this Mach number is larger than about three or four the particles have all turned their broadside to the stream, evidently controlled by inertia.

The orientation of a long body settling in a liquid under gravity is equivalent to the steady flow past a stationary long body. This latter problem has been treated in works of Ultman & Denn (1970), Joseph (1985), Crochet & Delvaux (1990), Hu & Joseph (1990) and Fraenkel (1988, 1991). These studies and related matters are discussed in J1990. The nonlinear studies were based on the upper convected Maxwell model, but the linearized studies were basically model independent. In the linearized problem the flow goes supercritical when the viscoelastic Mach number $M = U/c$ passes through one; the vorticity equation of the steady flow changes type from elliptic when $M < 1$ to hyperbolic when $M > 1$. In the supercritical case there is a Mach cone of vorticity. In the front of the cone there is a 'region of silence', actually potential flow with vortical flow in the cone behind the shock. In the nonlinear problem there can be a subcritical region near the body even when $M > 1$, as in transonic flow; but away from the body linearized dynamics will prevail. The supercritical transitions do seem to correspond to flow transitions observed in the experiments on the flow over wires reported by James (1967), James & Acosta (1970) and by Ambari, Deslouis & Tribollet (1984) as well as in the flow features observed in the experiments on flow over flat plates of Hermes & Fredickson (1967).

The experiments on anomalous transfer of heat and mass in the flow over small wires were carried out in dilute drag reducing solutions of polymers in water, say 10–100 p.p.m. of polyethylene oxide in water. The critical issue posed by these experiments is the comparison of the critical values of the velocity above which anomalous behaviour occurs with measured values of the wave speed. Some few values for wave speeds for very dilute solutions are presented in the tables at the end of J1990, but they are not reliable. We need to find the techniques to do reproducible measurements of wave speeds in dilute solutions. Gas dynamics would look good on paper, but only there, if we could not measure the speed of sound. Fortunately reliable measurements of the wave speeds of solutions in which tilt transitions occur can be made. In every one of many cases the transition commences when the fall velocity exceeds the wave speed, in all cases without exception.

Goldshtik, Zametalin & Shtern (1982) gave an interesting interpretation for the criterion for the onset of drag reduction in a Maxwell fluid. They said that there are two lengths to consider, a viscous length ν/u^* where ν is the kinematic viscosity and u^* is the friction velocity, and an elastic length λu^* where λ is the relaxation time. Onset occurs when the elastic length exceeds the viscous one.

$$\lambda u^* > \nu/u^*. \tag{1.1}$$

We can apply the same idea to the tilt transition by claiming onset when

$$\lambda U > \nu/U. \tag{1.2}$$

The question is what λ should be used. Our answer is that $\lambda = \nu/c^2$ which we get by measuring ν and c (shear wave speed) on our meter. Then, $M^2 = (U/c)^2 > 1$, correlating unrelated dynamic data from many different experiments.

All of the data including the values of dimensionless parameters have been collected in tabular and graphical form and are available upon request (Liu & Joseph 1993, hereinafter referred to as LJ1993).

2. Material and dimensionless parameters

The material parameters which were measured in the liquids used in the experiments are the density ρ, viscosity $\eta = k\dot{\gamma}^{n-1}$, where $\dot{\gamma}$ is the shear rate in reciprocal seconds, the climbing constant $\hat{\beta}$ measured on a rotating rod viscometer (Beavers & Joseph 1975) and wave speed c. To compute $\hat{\beta}$ from measured values of the climb we need the interfacial tension which we measured with a spinning drop tensiometer (Joseph *et al.* 1992*a*). The value of $\hat{\beta}$ is insensitive to a small change of surface tension (chapter 16 in J1990). Tables of material parameters will appear where they are first used.

The climbing constant $\hat{\beta}$ is related to the limiting (zero shear) value of the first and second normal stress differences

$$(n_1, n_2) = \lim_{\gamma \to 0} (N_1(\dot{\gamma}), N_2(\dot{\gamma}))/\dot{\gamma}^2, \tag{2.1}$$

by

$$\hat{\beta} = \tfrac{1}{2}n_1 + n_2. \tag{2.2}$$

The climbing constant,

$$\hat{\beta} = 3\alpha_1 + 2\alpha_2, \tag{2.3}$$

may also be expressed in terms of quadratic constants,

$$(\alpha_1, \alpha_2) = (-\tfrac{1}{2}n_1, n_1 + n_2), \tag{2.4}$$

of the second-order fluid. $\alpha_2/|\alpha_1|$ is the ratio of quadratic constants and

$$[\alpha_1, \alpha_2] = [-m, 2m-2]\hat{\beta}/(m-4) \tag{2.5}$$

where $m = 2\alpha_1/(2\alpha_1 + \alpha_2) = -n_1/n_2$ is the ratio of the first to second normal stress difference. It can be argued (§17.11 in J1990) that $m = 10$ is a reasonable value for our polymer solutions. Then

$$\frac{\alpha_2}{|\alpha_1|} = \left|\frac{2(1-m)}{m}\right| = 1.8 \tag{2.6}$$

is a constant and α_1 and α_2 are determined by the measured values of the climbing constant $\hat{\beta}$. We are going to assume (2.6) in all that follows. The value of n_1 we get from measuring $\hat{\beta}$ is not sensitive to the value of the ratio n_2/n_1 as long as n_2 is relatively small and negative (see §17.11 in J1990).

The measured value of the climbing constant together with the assumption that the second normal stress difference is $-\frac{1}{10}$ as large as the first, allows us to evaluate Roscoe's (1965) formula,

$$T_{11} - T_{22} = 3\dot{s}\eta_0 + 3(\alpha_1 + \alpha_2)\dot{s}^2, \tag{2.7}$$

for the extensional stress difference where $\dot{s}$ is the rate of stretching in the direction x_1 and η_0 is the zero shear viscosity. Using (2.6) and $\alpha_1 = -\frac{1}{2}n_1$ we get

$$T_{11} - T_{22} = 3\dot{s}\eta_0 + 1.2n_1\dot{s}^2. \tag{2.8}$$

The zero shear value of the first normal stress difference $n_1 = (2m/m-4)\hat{\beta} = \frac{10}{3}\hat{\beta}$ and the zero shear quadratic correction $4\dot{s}\hat{\beta}$ of Troutons viscosity, $3\eta_0$, increase with $\hat{\beta}$.

The device used to measure the wave speed c is a second generation wave speed meter which is basically a Couette device of the type described in Joseph, Narain & Riccius (1986*a*), Joseph, Riccius & Arney (1986*b*) and Appendix F of J1990. The new device has been simplified in various ways and it will be described in another publication. The values of measured wave speeds in this paper may be compared with the values listed in J1990 (pp. 701, 702) and the agreements are within the error bounds, approximately 30%. Certain theoretical issues with regard to wave speeds have not yet been resolved. The speeds we measured correspond to the shear wave speed $c = (G/\rho)^{\frac{1}{2}}$, where $G = \rho/\lambda$ is the shear modulus that one might expect to see in very soft rubbers, rather than to speeds of the order 10^5 cm/s which are expected in the high-frequency limit when the liquid responds as an elastic solid. The slow measured speeds presumably correspond to frequencies on a slowly varying portion of the storage modulus which may be approximated as a plateau. We do not believe there is a real plateau, so that different input frequencies should lead to different speeds. Moreover, the shear waves are dispersive so that we may see the spreading of any wave whose input is not a perfect step. In addition, the possible viscous effects of fast modes which have completely relaxed at the timescales of the experiments also need to be better understood. We are surprised more by the robustness of the measurements than by the scatter of the measurements. This may be due to the fact that the frequency of the impulse signal in our Couette meters may not excite greatly different speeds. And it is just the speeds which we measure on our meter which appear to correspond so well with dynamics in the problems of flow over bodies and delayed die swell as well as in the tilt angle transition reported here.

The study of supercritical flow around bodies can be expressed in terms of a Reynolds number Re and a Weissenberg (Deborah) number W. The Reynolds number is given by

$$Re = \frac{Ul}{\eta(\dot{\gamma})}, \tag{2.9}$$

where U is the terminal velocity and l is the hydraulic diameter (4 times the projected area over the projected perimeter where the projection is on the plane perpendicular to gravity). Formulae for l for flat, round and cone end cylinders are given in LJ1993.

The Weissenberg number will be defined by

$$W = \frac{\lambda U}{l}, \tag{2.10}$$

which is appropriate for models like Maxwell's with a single time of relaxation. For these models

$$Re\, W = \frac{U^2}{(\eta/\lambda\rho)} = \frac{U^2}{c^2} = M^2 \tag{2.11}$$

The relaxation time $\lambda = \eta/\rho c^2$ taken from wave speed measurements is much smaller than the values obtained on conventional rheometers which typically filter out the high-frequency response.

The parameters Re and W are convenient for studies in which hyperbolicity and change of type are not relevant. When change of type is an important issue, it is better to use M and either

$$E = \frac{\eta\lambda}{\rho l^2} \quad \text{(elasticity number)} \tag{2.12}$$

or W as the fundamental parameters. The parameters are related, $W = Re\, E$, $Re = M/E^{\frac{1}{2}}$.

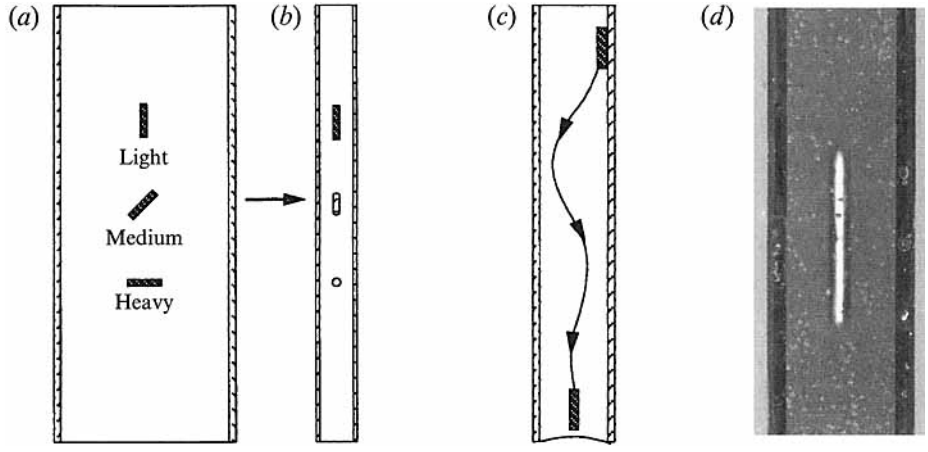

FIGURE 3. Cylinders always centre themselves to the plane midway between the closely spaced sidewalls no matter what the initial condition and the final orientation. (*a*) Front view. (*b*) Side view. (*c*) Cylinder centring. (*d*) Photograph.

Material	Density g/cm^3	Diameter *D*, inches	Length *L*, inches	Shapes
Plastic	1.32	0.1, 0.15, 0.25, 0.35, 0.4	0.4, 0.6, 0.8, 1.0	*f*, *c*, *r*
Teflon	2.18	0.25	0.4, 0.6, 0.8, 1.0	*f*, *c*, *r*
Aluminium	2.70	0.1, 0.15, 0.25, 0.35, 0.4	0.4, 0.6, 0.8, 1.0	*f*, *c*, *r*
Titanium	4.49	0.25	0.4, 0.6, 0.8, 1.0	*f*, *c*, *r*
Tin	7.29	0.1, 0.15, 0.25, 0.4	0.4, 0.6, 0.8, 1.0	*f*, *c*, *r*
Stainless steel	7.83	0.017, 0.25	0.4, 0.6, 0.8, 1.0	*f*, *c*, *r*
Brass	8.48	0.1, 0.15, 0.25, 0.3, 0.35, 0.4	0.4, 0.6, 0.8, 1.0	*f*, *c*, *r*
Lead	11.3	0.312	0.4, 0.6, 0.8, 1.0	*f*, *r*
Tungsten carbide	15.8	0.312	0.4, 0.6, 0.8, 1.0	*f*

TABLE 1. Test particles. The particles had cone ends, round ends and flat ends designated by *c*, *r* and *f* respectively

3. Description of the experiments

Particles were dropped in a liquid-filled channel, called a sedimentation channel. Three channels were used: two for sedimenting cylinders and one for sedimenting flat plates (which will be described in §4.4). The first two channels were much wider than they were deep. The one used for the constant temperature experiments has a gap of 0.44 in., is 6.5 in. wide and 25 in. high. A second channel which was used to test the effects of varying the temperature has a gap of 0.275 in., is 4 in. wide and 23 in. high. A heating mat was pasted on one side of this channel to facilitate uniform heating and the temperature of the mat could be controlled.

We used different test particles to vary the weight, size and shape as shown in table 1.

The motion of sedimenting particles in our three-dimensional bed is basically two-dimensional. The central axis of the cylinder always aligns itself in the plane midway between the closely spaced sidewalls, no matter what the initial condition (see figure 3).

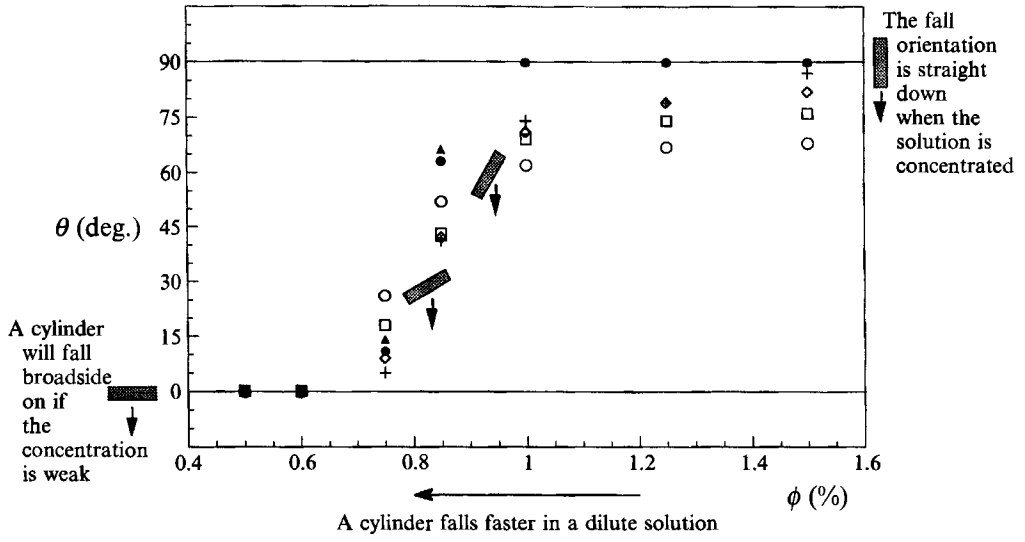

FIGURE 4. The effect of the concentration of Polyox in water ($T = 24$ °C) on the tilt angle for titanium cylinders ($D = 0.25$ in.). When $\theta = 0°$ the motion is dominated by inertia; when $\theta = 90°$ the motion is dominated by normal stresses. As the concentration increases the tilt angle θ becomes larger. ○, $L = 0.4$ in.; □, 0.6; ◇, 0.8, +1, for flat ends; ●, 0.8 (round ends); ▲, 0.8 (cone ends).

ϕ (%)	T (°C)	$\hat{\beta}$ (g/cm)	n_1 (g/cm)	c (cm/s)	η_0 (poise)	k	n
0.5	24	37.3	124	9.05	5.2	5.17	0.537
0.6	24	48.5	162	10.0	7.43	6.76	0.503
0.75	24	62.3	208	11.9	25.2	20.3	0.463
0.85	24	90.6	302	12.2	57.5	29.3	0.432
1	24	108	360	14.0	76.5	39.7	0.419
	35	105	360	—	—	—	—
	45	96.4	321	—	—	—	—
	54	90.4	301	—	—	—	—
1.25	24	117	389	17.2	112	64.2	0.393
1.5	24	132	440	20.3	204	101	0.378

TABLE 2. Properties of aqueous polyox (WSR-301, molecular weight 4×10^6)

Even a thin wire needle whose diameter (0.017 in.) is over 20 times smaller than the gap (0.44 in.) will centre itself in this way. The central position of particles is an effect of close or distant sidewalls. Apart from the drag, which we did not study, the motion of the cylinders in the central plane is apparently independent of the gap size. Tilted cylinders experience a side force and side drift, so that sedimentation channels must have a much greater breadth than depth. Small cylinders dropped in large tanks of circular cross-section behave exactly as they do in the beds with close sidewalls; the tilt action is localized in a vertical plane defined by the cylinder axis.

The effects of sidewalls are important in industrial applications, though these may be better modelled by particles in shear rather than sedimenting flows. For example, the positioning of particles in viscoelastic liquids used to fracture oil bearing reservoirs is important for maintaining open cracks to increase the conductivity of the reservoir after the liquid is withdrawn.

Velocities and tilt angles were measured with a Kodak Spin Physics SP2000 Motion

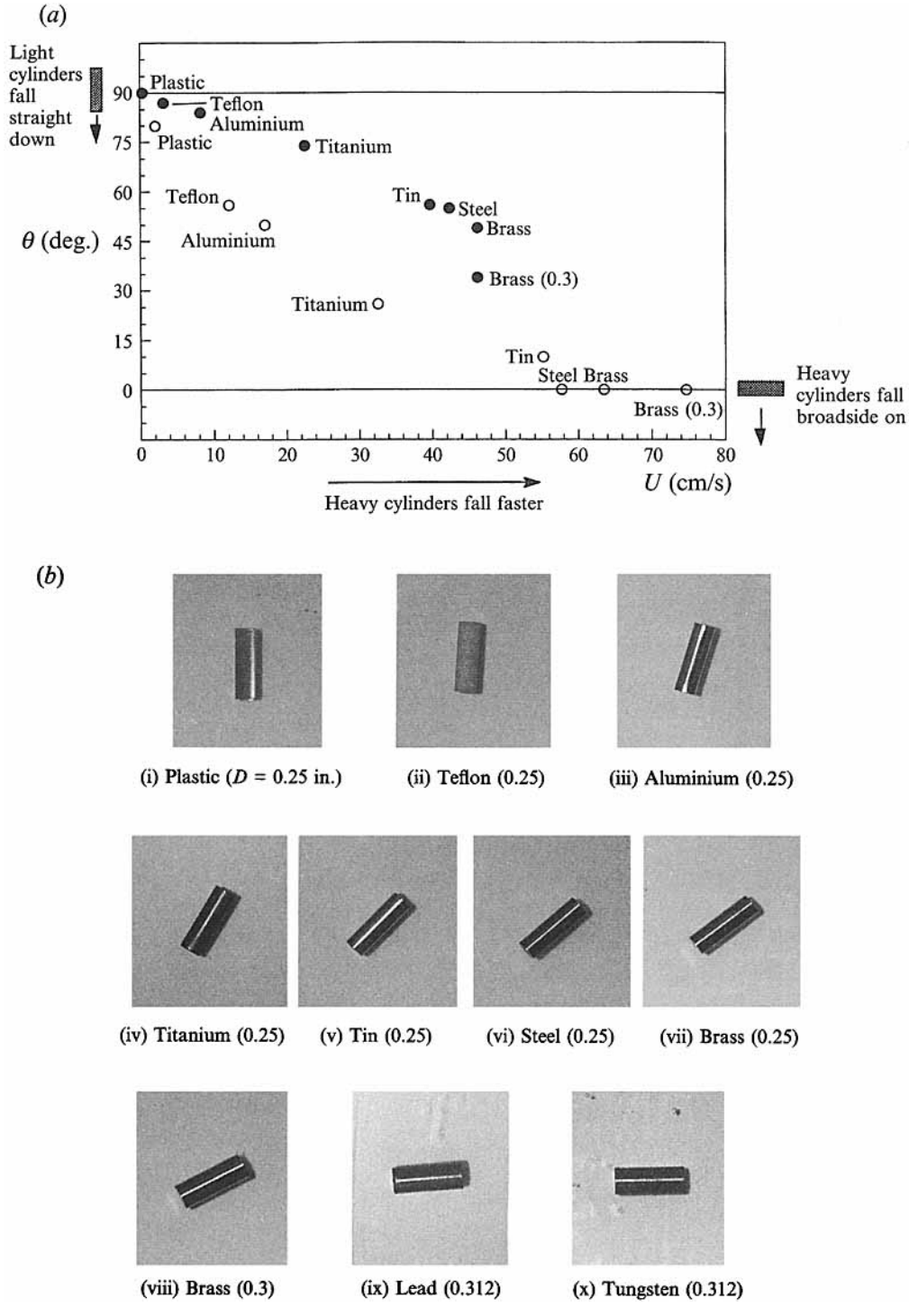

FIGURE 5. The effect of cylinder weight on the tilt angle ($T = 24$ °C). (*a*) Cylinders with same length $L = 0.4$ in. but different densities falling in ○, 0.75% and ●, 1.0% aqueous polyox solution. The heavier the cylinder, the smaller the tilt angle. (*b*) Shows how cylinders with $L = 0.8$ in. fall in 0.85% aqueous polyox solution.

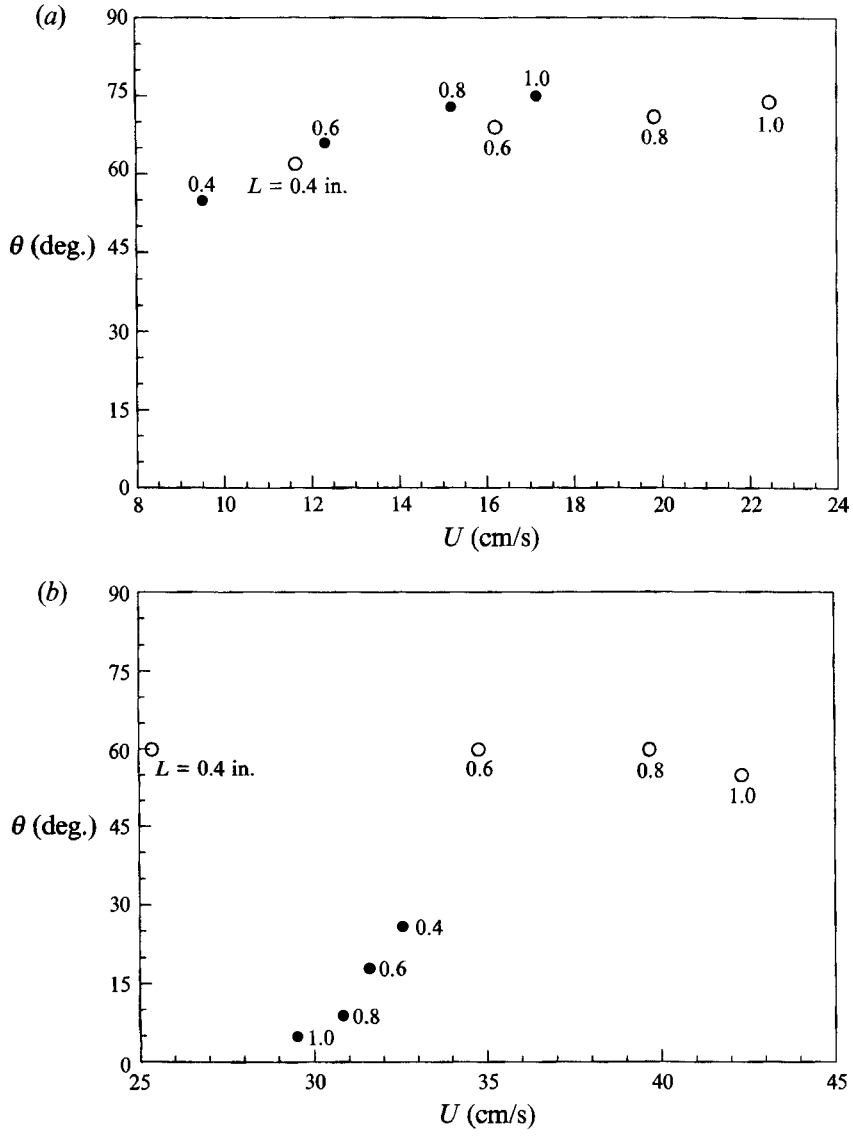

FIGURE 6. The effect of cylinder length on the tilt angle ($T = 24$ °C). (*a*) ○, titanium cylinders ($D = 0.25$ in.) in 1.0% aqueous Polyox and ●, brass cylinders ($D = 0.3$ in.) in 1.5% aqueous Polyox. (*b*) ○, steel cylinders ($D = 0.25$ in.) in 1.0% aqueous Polyox and ●, titanium cylinders ($D = 0.25$ in.) in 0.75% aqueous Polyox.

Analysis System which can take pictures at 2000 frames per second (f.p.s.). The image is replayed at a speed of 60 f.p.s. Images can also be played forward or backward at the rates of $\frac{2}{3}$, 1, $\frac{3}{2}$ or 3 f.p.s., or one frame at a time. There are movable reticle lines which allow spatial measurements of the image. The elapsed time may be observed while a recording is being made and replayed. These functions allow one to measure the fall speed and tilt angle of sedimenting particles.

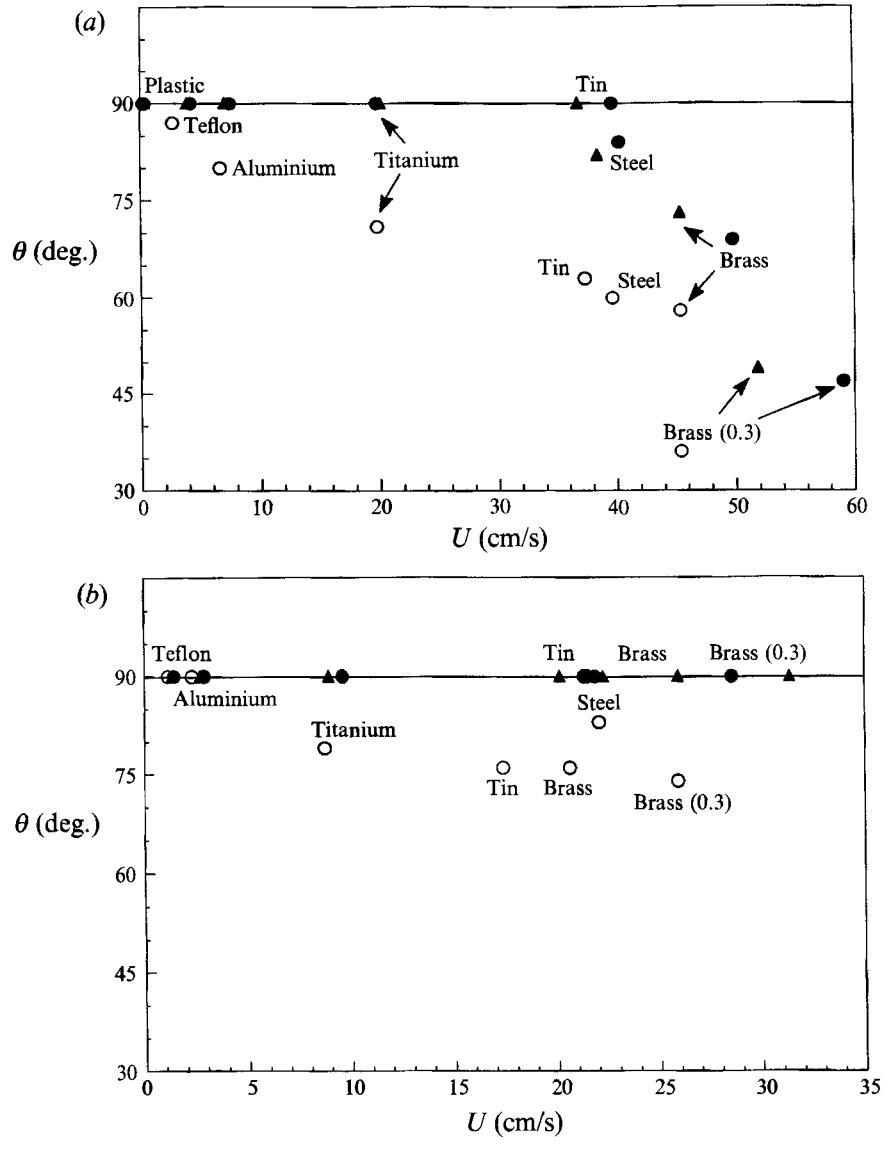

FIGURE 7(*a*, *b*). For caption see facing page.

4. Tilt angle transition

In this section we catalogue our observations of the tilt angle transition, from straight-down when normal stresses dominate to broadside-on when inertia dominates. We will look at the effects of changing the concentration, fall speed, particle length and diameter, particle shape and liquid temperature.

4.1. *Polyox (WSR 301) in water*

The concentration ϕ in percentage by weight of the polymer was varied from 0.5 to 1.5. Our heaviest particles (tungsten carbide) would not fall fast enough to see the effects of inertia on the tilt transition in solutions more concentrated than 1.5%. (The viscoelastic Mach number for very concentrated solutions is always well below one and the particles would not fall broadside-on.) Table 2 gives the values of the material

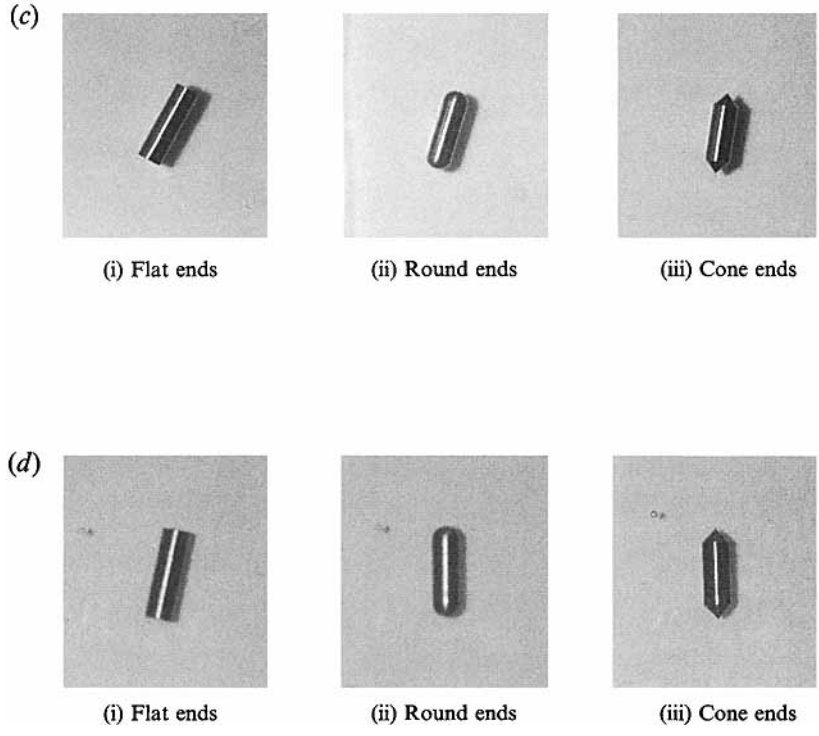

FIGURE 7. The effect of cylinder shape on the tilt angle ($T = 24$ °C). (*a*) Cylinders with same length $L = 0.8$ in. but with flat ends, round ends and cone ends, respectively, falling in 1.0% Polyox/water solution, (*b*) the same cylinders falling in 1.25% solution, (*c*) and (*d*) brass cylinders falling in 1.0% and 1.5% solutions. ○, flat ends; ●, round ends; ▲, cone ends.

parameters, such as the rod climbing constant $\hat{\beta}$, the zero shear value of the first normal stress difference n_1, the shear wave speed c, the zero shear rate viscosity η_0 and the power law constants k and n.

The 0.5% Polyox/water solution is weakly viscoelastic. It climbs a rotating rod (see table 2). In the sedimentation experiments, the 0.5% solution behaves as if Newtonian: all particles sediment broadside-on. Since the viscosity of this solution is low, the fall speed is high. Viscoelastic effects are already strongly apparent in the 0.6% solution.

In figure 4 we have plotted the variation of the tilt angle with concentration for titanium cylinders. In all cases the tilt angle transition is a smooth function of concentration with broadside-on configurations ($\theta = 0°$) dominant at low concentrations where inertia dominates and straight-down configurations ($\theta = 90°$) dominant at high concentrations where non-Newtonian normal stresses dominate.

Heavier cylinders are increasingly dominated by inertia, tending to settle broadside-on. This is evident in figure 5 in which the tilt angle is plotted as a function of fall velocity for different cylinders in solutions with different concentrations. Even the heavy cylinders fall slowly in concentrated, viscous solutions and are dominated by non-Newtonian effects in which memory, shear thinning and normal stresses are implied.

We turn now to the effect of systematic changes in the length of the cylinders on the tilt angle. Four different lengths of 0.4 in., 0.6 in., 0.8 in. and 1.0 in. were tested. Figure 6(*a*) shows that longer cylinders typically fall at a larger tilt angle. However, in lower concentration solutions normal stress effects are weak, so that when the fall speeds of

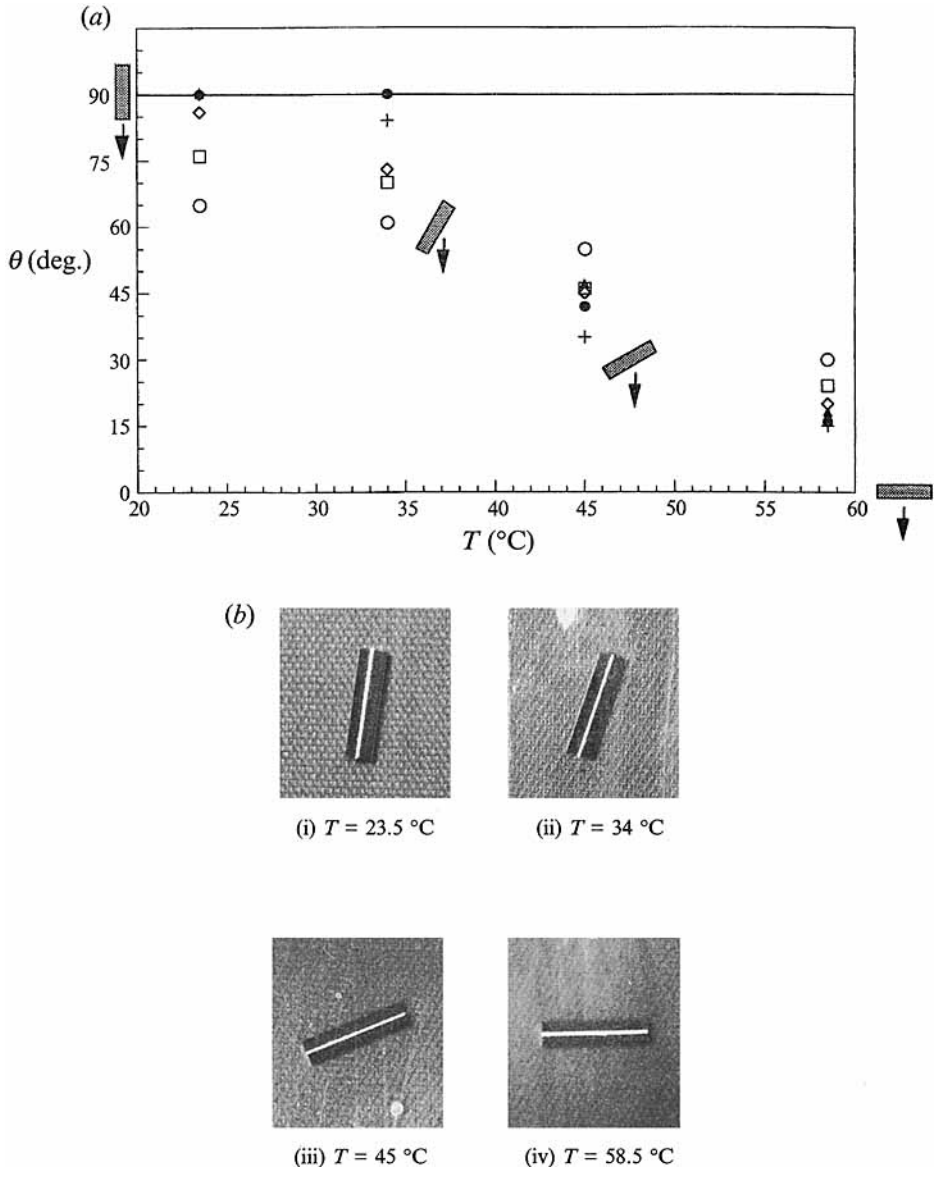

FIGURE 8. The effect of liquid temperature on the tilt angle. (*a*) Tin cylinders ($D = 0.25$ in.) falling in 1.0% Polyox/water solution at different temperatures. L (in.) Flat ends: ○, 0.4; □, 0.6; ◇, 0.8; +, 1.0. Round ends: ●, 0.8. Cone ends: ▲, 0.8. (*b*) A brass cylinder with $(D, L) = (0.25, 1.0)$ in. in 1.0% Polyox/water solution at different temperatures. As the temperature increases, the tilt angle decreases.

particles are high, their tilt angles are affected more by their weights than by their lengths. Then the longer cylinders may have smaller tilt angles, as shown in figure 6(*b*). One may also verify, from figure 6(*b*), that when the normal stresses are relatively strong, as in the 1.0% Polyox/water solution, and the fall speeds of cylinders are high, the tilt angles are determined by the joint effect of cylinder length and weight. When normal stresses are weak, solutions with concentrations lower than 0.75%, the tilt angle is affected more by cylinder weight than length. A longer cylinder may have a

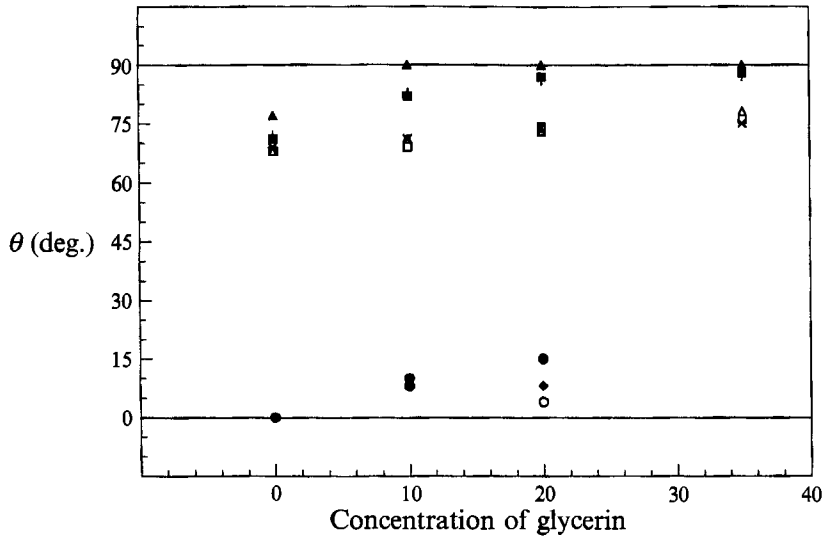

FIGURE 9. The effect of the concentration of glycerin in 0.8% Polyox in glycerin/water solutions on the tilt angle ($T = 24$ °C). The lead and tungsten carbide particles have a diameter of 0.312 in. and the others have a diameter of 0.25 in. The lengths of the particles are all 0.8 in. The particles have flat ends and round ends designated by (f): △, tin; ×, steel; □, brass; ○, lead; ◆, tungsten. (r): ▲, tin; +, steel; ■, brass; ●, lead, respectively. As the concentration of glycerin increases, the particles fall slower decreasing the effects of inertia, and increasing the tilt away from the horizontal orientation $\theta = 0°$.

0.8% Polyox in:	$\hat{\beta}$ (g/cm)	n_1 (g/cm)	c (cm/s)	η_0 (poise)	k	n
Water	79.7	266	12.7	45.5	13.3	0.498
90% water/10% glycerin	68.9	230	14.0	57.6	15.6	0.492
80% water/20% glycerin	81.3	271	14.6	65.1	17.4	0.489
65% water/35% glycerin	93.6	312	17.0	86.2	21.7	0.486

TABLE 3. Properties of polyox (WSR301) in glycerin/water solutions

lower fall speed (figure 6*b*) because it has a smaller tilt angle and experiences a greater drag.

The tilt angle of a cylinder is also affected by the cylinder shape. The cylinders with round ends and cone ends always align with gravity better than the ones with flat ends (see figure 7 and figure 4). Forces at sharp corners tilt the cylinder axis away from the vertical ($\theta = 90°$) even when inertial effects are small.

Figure 8 shows the effect of temperature on the tilt angle. The effect of increasing the temperature is equivalent to the effect of decreasing the concentration of the solution, as is evident already from table 2.

In §5 we shall organize the data on the tilt angle transitions in the frame of the dimensionless variables defined in §2. We shall see that this transition from straight-down orientations when the viscoelastic Mach numbers are less than one to broadside-on orientations when the Mach numbers are greater than a number between one and four, may be explained as a change of type.

We also tested a very small diameter cylinder, $(D, L) = (0.017, 0.8)$ in. When the thin cylinder is dropped in 1.5% aqueous Polyox with its axis perpendicular to gravity it

Material	D (in.)	θ	U	Re	M	λ	E	W
Plastic	0.1	90	0.47	0.016	0.03	0.026	2.95	0.048
	0.15	90	0.78	0.042	0.05	0.025	1.24	0.052
	0.25	90	1.34	0.121	0.08	0.025	0.441	0.053
	0.25	90	1.09	0.094	0.07	0.026	0.480	0.045
(f)	0.25	90	1.08	0.093	0.06	0.026	0.482	0.045
	0.35	90	0.98	0.109	0.06	0.029	0.289	0.031
	0.4	90	0.99	0.123	0.06	0.029	0.232	0.029
Teflon	0.25	90	8.49	1.21	0.51	0.016	0.176	0.213
	0.25	90	7.54	1.03	0.45	0.017	0.190	0.197
(f)	0.25	90	7.19	0.96	0.43	0.017	0.199	0.192
Aluminium	0.1	90	4.01	0.241	0.24	0.015	0.990	0.239
	0.15	90	8.02	0.800	0.48	0.014	0.360	0.288
	0.25	90	14.9	2.59	0.89	0.013	0.119	0.309
	0.25	90	14.4	2.45	0.86	0.013	0.123	0.301
(f)	0.25	90	13.1	2.16	0.78	0.014	0.132	0.284
	0.35	53	18.3	5.07	1.09	0.015	0.046	0.235
	0.4	31	16.8	5.04	1.01	0.016	0.040	0.201
Titanium	0.25	8	20.0	5.15	1.20	0.014	0.054	0.278
	0.25	4	18.7	4.70	1.12	0.014	0.057	0.266
	0.25	0	20.0	5.15	1.20	0.014	0.054	0.278
(f)	0.25	13	20.0	5.15	1.19	0.014	0.054	0.277
(f)	0.25	11	18.5	4.65	1.11	0.014	0.057	0.264
Tin	0.1	85	27.3	4.74	1.63	0.007	0.119	0.560
	0.1	88	27.2	4.59	1.63	0.006	0.126	0.580
	0.15	4	19.7	3.90	1.18	0.012	0.091	0.355
	0.25	0	41.6	14.6	2.49	0.010	0.029	0.425
	0.25	0	39.7	13.6	2.37	0.011	0.031	0.415
(f)	0.25	0	37.4	12.2	2.23	0.011	0.034	0.410
	0.4	0	60.5	30.2	3.62	0.010	0.014	0.433
Steel	0.25	0	45.4	16.6	2.71	0.010	0.027	0.444
	0.25	0	40.1	13.8	2.40	0.010	0.030	0.417
(f)	0.25	0	43.0	15.0	2.57	0.010	0.029	0.441
Brass	0.1	90	33.9	7.04	2.03	0.004	0.083	0.583
	0.15	0	24.7	5.40	1.47	0.011	0.075	0.403
	0.25	0	48.8	18.6	2.92	0.009	0.025	0.460
	0.25	0	47.4	17.7	2.83	0.010	0.026	0.453
(f)	0.25	0	44.6	15.8	2.67	0.010	0.028	0.448
	0.3	0	60.5	27.5	3.62	0.009	0.017	0.476
	0.3	0	57.7	25.6	3.45	0.009	0.018	0.466
(f)	0.3	0	54.0	22.7	3.23	0.009	0.020	0.460
	0.35	0	68.6	35.2	4.11	0.009	0.014	0.479
	0.4	0	72.6	39.9	4.34	0.009	0.012	0.472

TABLE 4. Tilt angle response of sedimenting cylinders in 2% aqueous polyacrylamide (Cyanamer N-300 LMW) at room temperature. All the particles have the same length $L = 0.8$ in. Most cylinders have round ends except some with flat ends designated by (f)

will sediment very slowly and gradually turn to the straight-down position. In this case $M \ll 1$ and $Re \ll 1$. When it falls in 0.5% aqueous Polyox, it will turn its broadside to the stream with $(M, Re) \sim (2, 1.6)$ consistent with a change of type.

4.2. *Polyox in glycerin/water solutions*

Table 3 gives the values of the material parameters of 0.8% Polyox (WSR301) in glycerin/water solutions. The tilt angle of cylinders of length 0.8 in. falling in these solutions is plotted against the concentration of glycerin in figure 9. Increasing the

Liquid	Plate no.	θ	U	Re	M
2% aqueous polyacrylamide	1	90	3.14	0.111	0.188
	2	90	16.0	1.66	0.960
	3	80	16.5	3.46	0.985
	4	0	19.7	9.01	1.18
1.5% aqueous Polyox	3	90	1.75	0.013	0.086
	4	90	3.87	0.055	0.191
0.85% aqueous Polyox	1	90	2.04	0.043	0.168
	2	90	7.62	0.306	0.627
	3	90	14.9	1.11	1.23
	4	80	21.9	3.96	1.80
	5	70	27.9	7.20	2.30
0.75% aqueous Polyox	1	90	2.49	0.077	0.210
	2	90	12.0	0.772	1.01
	3	90	17.6	1.79	1.48
	3	90	21.0	2.34	1.77
	4	75	25.2	7.31	2.12
	4	80	26.2	6.77	2.20
	5	50	33.4	14.7	2.81
0.60% aqueous Polyox	1	90	5.81	0.733	0.579
	2	10	11.0	8.15	1.10
	3	0	16.8	15.4	1.67
	4	0	28.2	33.6	2.81
	5	0	28.5	34.4	2.84
0.50% aqueous Polyox	1	90	7.84	1.30	0.866
	2	0	16.2	17.7	1.79
	3	0	21.5	27.1	2.38
	4	0	30.2	44.7	3.34
	5	0	30.6	45.7	3.38

TABLE 5. Sedimentation of rectangular plates in a three-dimensional channel

glycerin content in the solution with 0.8% polyox is like increasing the percentage of polyox in an aqueous solution.

4.3. 2% *aqueous polyacrylamide*

The tilt angle response in the experiments on sedimentation of cylinders with length of $L = 0.8$ in. in the 2% aqueous polyacrylamide solution is described in table 4. The properties of 2% aqueous polyacrylamide (Cyanamer N-300 LMW, molecular weight 5×10^6) at room temperature are as follows: $\hat{\beta} = 96.4$ g/cm, $n_1 = 321$ g/cm, $c = 16.7$ cm/s and $\eta_0 = 9.5$ poise. The shear viscosity is fitted to the following correlation:

$$\eta = 8.12 - 3.24 \log \dot{\gamma}$$

where $\dot{\gamma}$ is the shear rate in the range of values occurring in this experiment.

4.4. *Sedimentation of flat plates*

We also dropped some rectangular plates in a three-dimensional channel of round cross-section of diameter 2.76 in. and depth 29 in. The experimental data are shown in table 5. The plates used in the tests are: (i) aluminium (length, width, thickness) = (1.161, 0.752, 0.026) in.; (ii) brass (1.161, 0.736, 0.02); (iii) steel (1.169, 0.752, 0.035); (iv) stainless steel (1.177, 0.752, 0.061); and (v) stainless steel (1.205, 0.752, 0.061). The lighter plates fall straight-down, the heavier ones fall broadside-on.

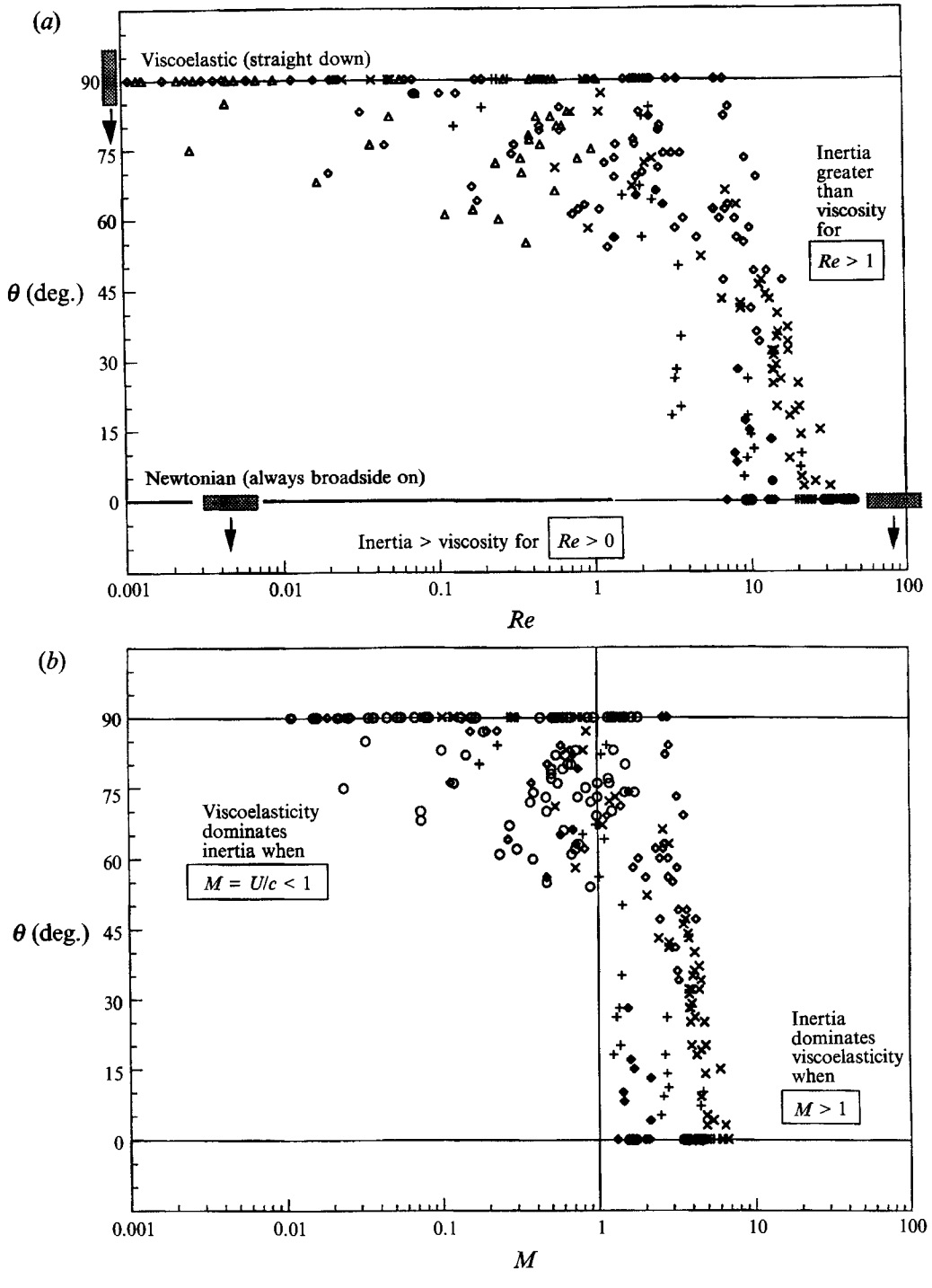

FIGURE 10(*a*, *b*). For caption see facing page.

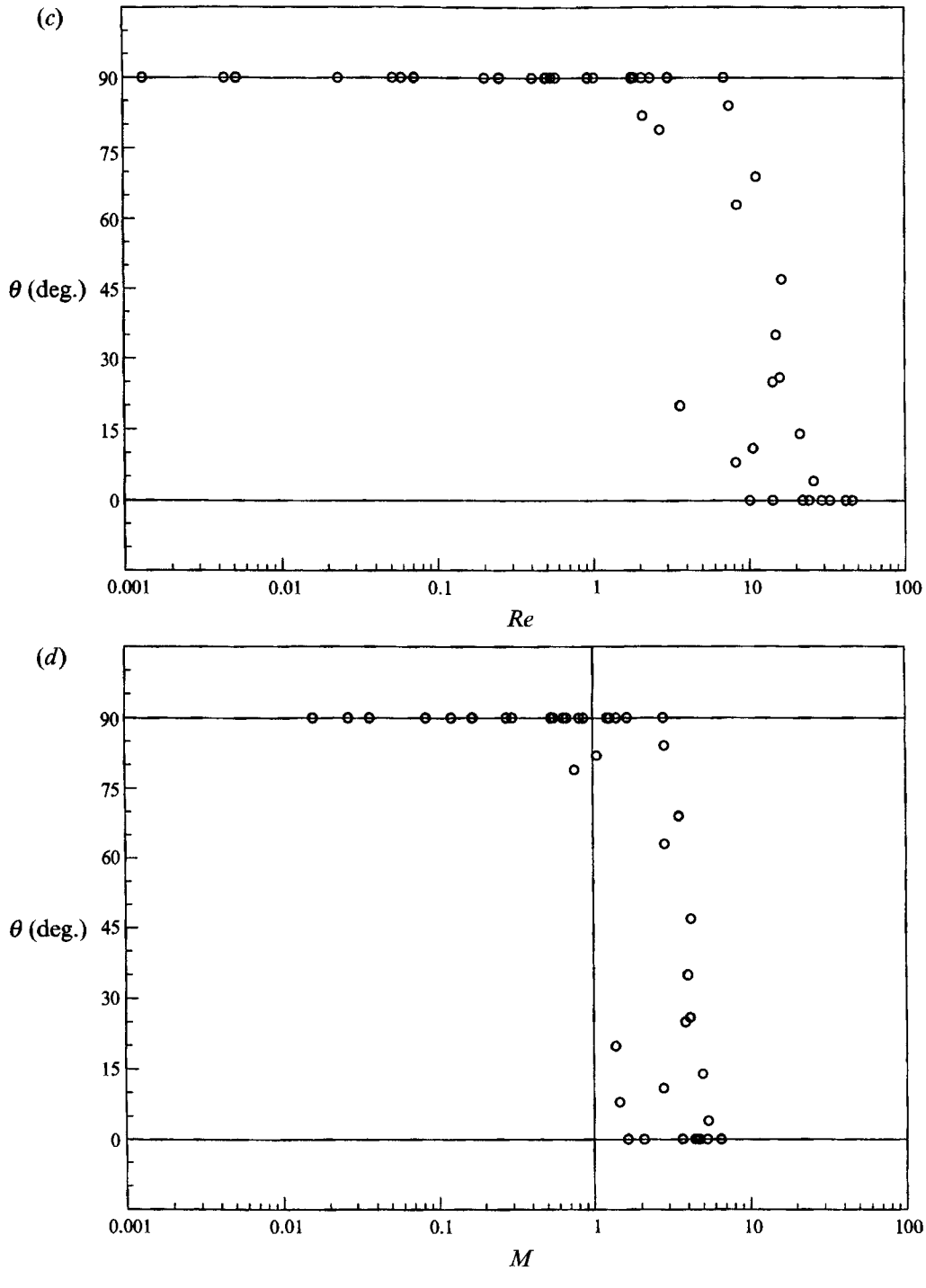

FIGURE 10. (*a*) Tilt angle θ *vs.* Reynolds number *Re* and (*b*) θ *vs.* Mach number *M* for all the data, cylinders of all lengths (diameters are 0.25 in. except the lead and tungsten carbide cylinders with diameter of 0.312 in.), shapes and weights in polyox/water solutions: △, 1.5%; ○, 1.25%; ◇, 1%; ×, 0.85%; +, 0.75%; ◆, 0.6%; ●, 0.5%. (*c*) θ *vs.* *Re* and (*d*) θ *vs.* *M* for cylinders with round ends and $L = 0.8$ in. only in polyox/water solutions of various concentrations.

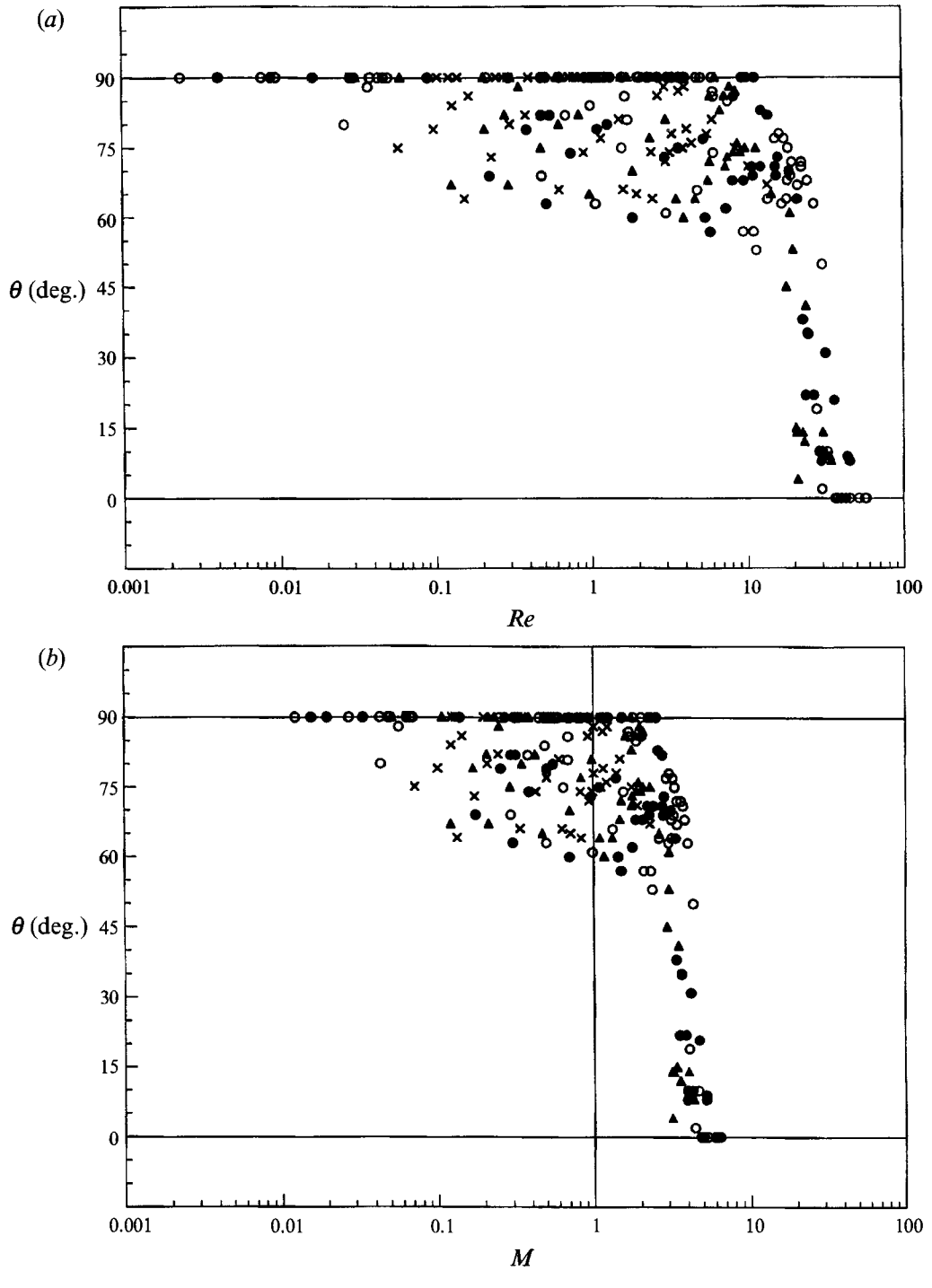

FIGURE 11(*a*, *b*). For caption see facing page.

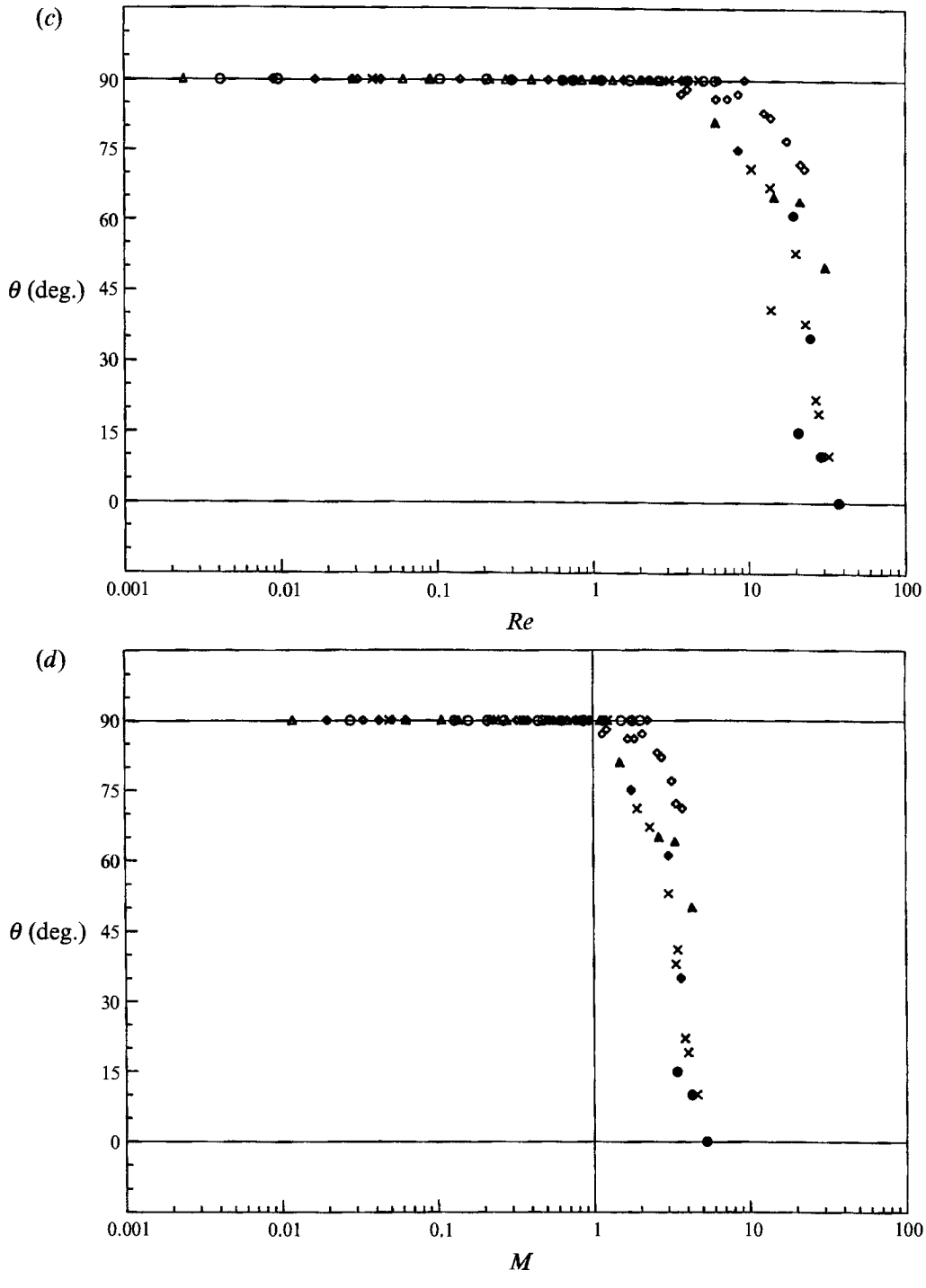

FIGURE 11. (*a*) Tilt angle θ *vs.* Reynolds number *Re* and (*b*) θ *vs.* Mach number *M* for all the data, cylinders of all lengths, diameters, shapes and weights in 0.8 % polyox in glycerin and water solutions: ○, 100 % water; ●, 10 % glycerin/90 % water; ▲, 20 % glycerin/80 % water; ×, 35 % glycerin/65 % water. (*c*) θ *vs. Re* and (*d*) θ *vs. M* for cylinders with round ends and $L = 0.8$ in. only: △, $D = 0.1$ in.; ○, 0.15; ◇, 0.25; ▲, 0.3; ●, 0.312; ◆, 0.35; ×, 0.4.

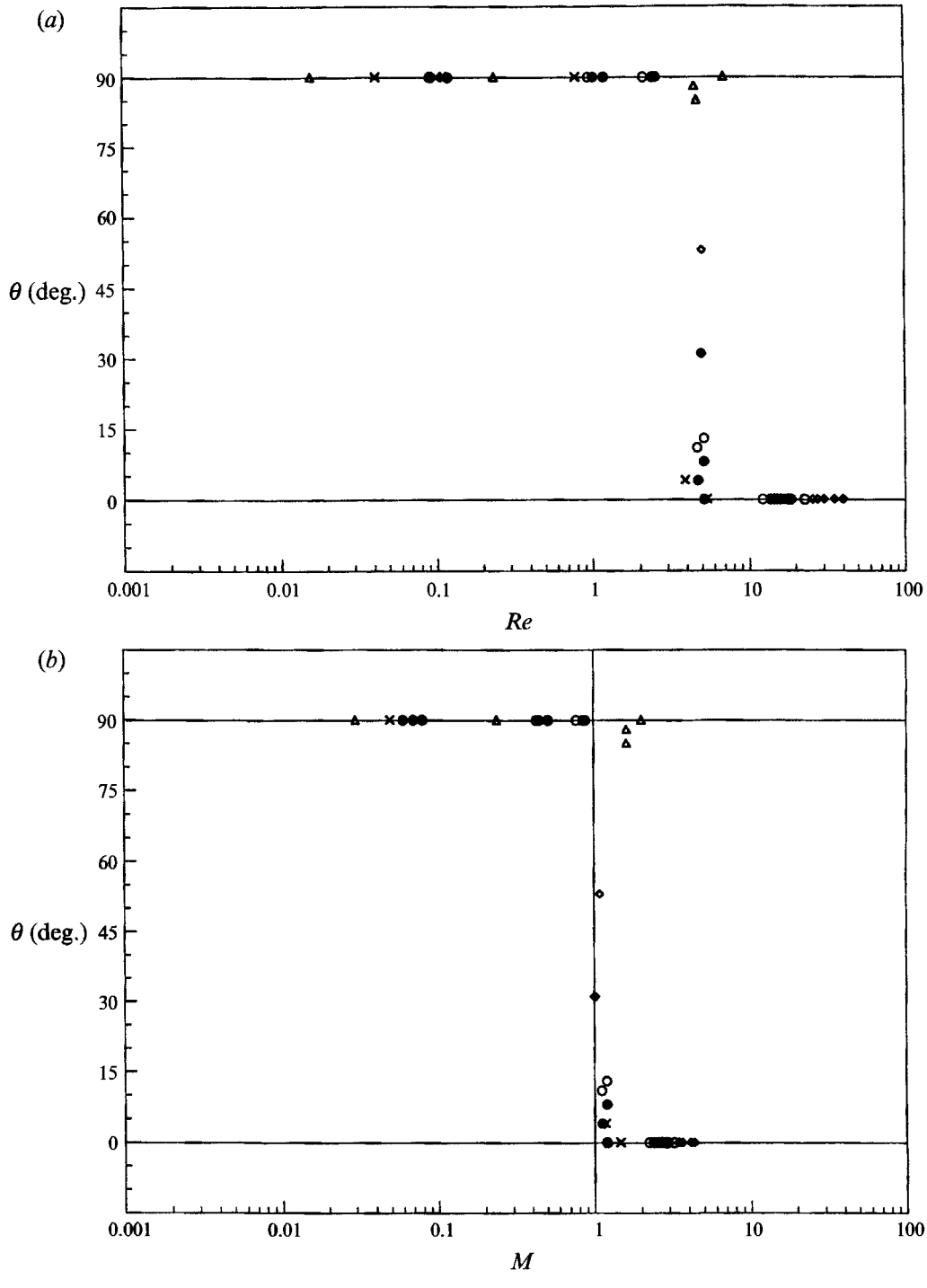

FIGURE 12. (*a*) Tilt angle θ *vs.* Reynolds number *Re* and (*b*) θ *vs.* Mach number *M* for cylinders with $L = 0.8$ in. (most with round ends) in 2% aqueous polyacrylamide: △, $D = 0.1$ in.; ×, 0.15; ●, 0.25; ○, 0.25 (flat ends); ◇, 0.35; ◆, 0.4.

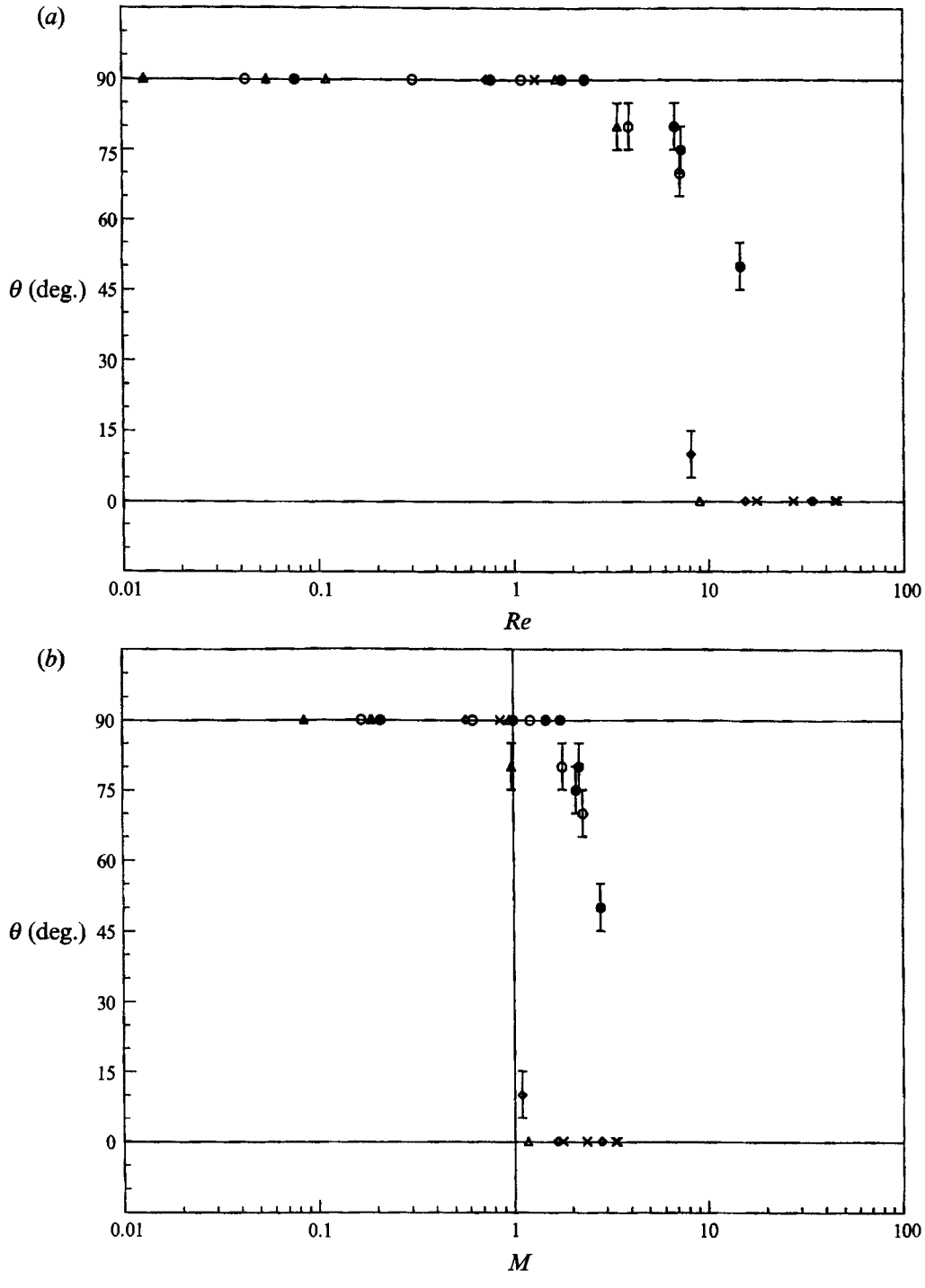

FIGURE 13. (*a*) Tilt angle θ *vs.* Reynolds number *Re* and (*b*) θ *vs.* Mach number *M* for rectangular plates in different aqueous polymer solutions: △, 2% polyacrylamide; ▲, 1.5% polyox; ○, 0.85% polyox; ●, 0.75% polyox; ◇, 0.6% polyox; ×, 0.5% polyox.

5. Critical Mach and Reynolds numbers

In this section we shall show how the tilt angle transition correlates with the viscoelastic Mach number and the Reynolds number. The Reynolds number is defined by (2.9) and we used the viscosity at the effective rate of shear $\dot{\gamma} = U/l$.

Cylinders in Newtonian liquids turn broadside-on when $Re > 0.1$ and will eventually turn broadside-on for any $Re > 0$. No matter how small Re may be, the orientation of the body will eventually be determined by inertia. Bodies with fore and aft symmetry are torque free when settling in Stokes flow, so that the torques due to inertia, no matter how small, are unopposed.

In contrast, cylinders which fall straight-down in viscoelastic fluids are dominated by normal stresses when Re is smaller than some finite value of order unity which we shall designate in a loose manner by saying that $Re < 1$. This is not like the fall of cylinders in Newtonian fluids because inertia does not control the orientation of a falling cylinder as long as $Re < 1$. To make the cylinder turn broadside-on we need to have $Re > 1$, that is, the inertial forces are greater than the viscous forces. This is condition one for tilting.

The second condition, $M > 1$ for tilting, tells us that the elastic length λU is larger than the viscous length ν/U, where $\lambda = \nu/c^2$. The Mach number criterion is motivated by theory (J1990) which shows that when $M > 1$, waves of vorticity (shear waves) cannot propagate upstream into the region at rest. Asymptotically upstream, the vorticity is confined to the region behind a shock which terminates in a Mach cone and the flow in front of the shock is irrotational. It is possible that the potential flow at the front of the body is a source of the turning couples which produce the tilt angle transition.

More detailed understanding of the inertial mechanisms which turn the body in supercritical flow will require nonlinear analysis, probably in the form of a computer-aided analysis. In the case of the related problem of plane flow past a circle, Crochet & Delvaux (1990) (see J1990) showed that supercritical regions could develop locally even with $M < 1$, as in transonic flow.

The argument we have constructed to support the notion that inertia dominates the tilting of long bodies across the stream when $Re > 1$ and $M > 1$ will be clearer if we factor out tilting due to shape. Cylinders with flat ends, unlike the cylinders with round ends and cone ends, almost never fall with their axis perfectly aligned with gravity. Figures 4 and 7 as well as figure 4 in the paper by Joseph *et al.* (1992*b*), show that the cylinders with round ends and cone ends fall more perfectly straight. Even flat rectangular plates, which are falling with their broadside parallel to gravity, tilt in the plane of their motion, as in figure 2.

To factor out shape tilting we shall present Mach number data first with the flat end cylinders, then without them. Possible mechanisms for shape tilting will be considered in the discussion in §6.

Figures 10–13 show, respectively, the tilt angle θ *vs.* Reynolds number Re and θ *vs.* Mach number M for the sedimentation of cylinders in aqueous Polyox solutions, in 0.8% Polyox in glycerin and water solutions, in 2% aqueous polyacrylamide, and the sedimentation of flat plates.

6. Discussion

The results obtained in this paper are direct measurements independent of constitutive hypotheses. The experiments pose a number of theoretical questions: what

is the nature of the torques which will keep a long particle aligned with gravity when $Re < 1$ and $M < 1$? What are the mechanisms which produce small tilt angles (shape tilting) between the axis of cylinders and plates with sharp edges when $Re < 1$ and $M < 1$? What are the mechanisms of inertial tilting from straight-down to broadside-on as Re and M are increased past one? What can be said about sedimentation is semidilute solutions bridging the gap between Newtonian and non-Newtonian fluids? What is the relationship between the natural orientation of sedimenting cylinders and the flow induced symmetries of sedimenting spheres?

The perturbation analyses of Leal (1975) and Brunn (1977) show that the mechanisms which keep a long body aligned with gravity when $Re < 1$ and $M < 1$ can be found in second-order viscoelasticity, perturbing rest. We have already noted that shear thinning is a third-order effect which obviously cannot effect turning at second order. The aforementioned authors did not consider the effects of inertia so that one might think that the orientation effects could be determined from the simultaneous perturbation with inertia and viscoelasticity. This idea was expressed by a critical reader as follows 'when both inertia and non-Newtonian effects are present, they tend to compete, and when the magnitudes of the two are of the same size, the particle rotates to an intermediate orientation where the two torque contributions cancel. This can occur even when the two effects are each very weak, i e for both $Re \ll 1$ and $W \ll 1$.' It is a good idea to study the competition of inertia and viscoelasticity by perturbations, and we are pursuing the idea. Even though perturbations cannot explain the results of our experiments because $Re\, W = M^2 > 1$ for tilting, we cannot conclude that similar behaviour might not be possible for combinations of smaller Re and W.

An extensional flow mechanism might appear in slow flow. A mathematical argument from the theory of slow potential flows is very suggestive. This argument builds on the situation described in figure 1. Readers may have reservations about applying the theory of potential flow to the kind of rheology of slow, slowly varying flows which leads to second-order theory. In the present case, we shall consider extensional flow. This is a special potential flow which is a universal solution of the dynamic equations. The extra stress in extensional flow is uniform in space and the spatially constant components of stress are model dependent. But since the divergence of the extra stress vanishes, the compatibility condition for the existence of a Bernoulli or pressure function is satisfied (see Joseph & Liao 1993).

It will not generally be possible to satisfy the boundary conditions on our cylinders with extensional flow. The fact that extensional flows are frequently considered by rheologists in circumstances where the aforementioned reservations hold could be cited as a kind of justification or it may mean simply that we are just following a corpus of wrong works presently propagating through the rheological literature. We present no justification for the analysis given below other than to say that we are going to assume that extensional slow flows at the points of stagnation of the corresponding potential flow are possible in some approximate sense and see where this assumption leads.

Joseph (1992) has shown that every potential flow is a solution of the equation of motion for second-order fluid with stresses given by

$$\sigma_{ij} = -[C+\hat{\beta}\phi_{,il}\phi_{,il}-\rho\phi_{,t}-\rho\tfrac{1}{2}|\boldsymbol{u}|^2]\,\delta_{ij} + 2[\eta+\alpha_1(\partial_t+\boldsymbol{u}\cdot\nabla)]\,\phi_{,ij}+4(\alpha_1+\alpha_2)\,\phi_{,il}\phi_{,lj}, \quad (6.1)$$

where σ_{ij} is the active dynamic stress, C is a Bernoulli constant. In general, potential flow cannot satisfy no-slip conditions at solid walls. And potential flow solutions of more general models of a viscoelastic fluid are not possible even when the boundary conditions are ignored. The streamlines in potential flows are determined by the

prescribed values of the normal component of velocity. You cannot see the effects that changing the values of the material parameters have on the values or distribution of the velocity in a potential flow. Potential flows of viscous fluids exist outside boundary-layer regions and separated regions behind bluff bodies. The position of the theory of potential flow in the dynamics of viscoelastic liquids, however, is not yet understood.

The case of flow at the stagnation points of a body in steady flow is of special interest. The steady streaming past a stationary body is equivalent, under a Galilean transformation, to the steady motion of a body in a fluid at rest. The quiescent streaming potential flow $(U,0,0)$ of a fluid near a point $(x_1,x_2,x_3)=(0,0,0)$ of stagnation is a purely extensional motion with principal rates of stretching

$$[\lambda_1,\lambda_2,\lambda_3]=U/l\dot{s}[2,-1,-1], \tag{6.2}$$

where $\dot{s}$ is half the dimensionless rate of stretching in the x_1-direction, l is the scale of length and

$$[u_1,u_2,u_3]=U/l\dot{s}[2x_1,-x_2,-x_3]. \tag{6.3}$$

In this case, $C=\frac{1}{2}\rho U^2$, and we have

$$\begin{bmatrix}\sigma_{11}&0&0\\0&\sigma_{22}&0\\0&0&\sigma_{33}\end{bmatrix}=\tfrac{1}{2}\rho U^2\left[\dot{s}^2\frac{4x_1^2+x_2^2+x_3^2}{l^2}-1\right]\begin{bmatrix}1&0&0\\0&1&0\\0&0&1\end{bmatrix}+2\eta\frac{U}{l}\dot{s}\begin{bmatrix}2&0&0\\0&-1&0\\0&0&-1\end{bmatrix}$$
$$+2\frac{U^2}{l^2}\dot{s}^2\begin{bmatrix}-\alpha_1+2\alpha_2&0&0\\0&-7\alpha_1-4\alpha_2&0\\0&0&-7\alpha_1-4\alpha_2\end{bmatrix} \tag{6.4}$$

At the stagnation point itself

$$\sigma_{11}=-\tfrac{1}{2}\rho U^2+4\eta\,U/l\dot{s}+2(2\alpha_2-\alpha_1)\,U^2/l^2\dot{s}^2. \tag{6.5}$$

Since $\alpha_1<0$ and $\alpha_2>0$, then $2\alpha_2-\alpha_1=\frac{5}{2}n_1+2n_2>0$ and the normal stress term in (6.5) is positive independent of the sign of $\dot{s}$, but $4\eta\dot{s}$ is negative at the front side of a falling body and is positive at the rear (see figure 1). This is a new manifestation of the competition between inertia and normal stress, which may play a role in the flow-induced anisotropy. In practice, we would not expect the symmetrical streamlines predicted by potential flow, but the normal stresses that are generated in the non-separated regions of flow around bodies may play an important role in the turning of long bodies and in the chaining of spherical bodies.

It is necessary to draw attention to the fact that the results just established are actually model independent and apply universally for slow, slowly varying motions (retarded motions of Coleman & Noll 1960) of any simple fluid. All models of a simple fluid have a pressure function in extensional flow (Joseph & Liao 1993). For example, the extra stress in the extensional flow of an upper convected Maxwell model,

$$\lambda\overset{\nabla}{\boldsymbol{\tau}}+\boldsymbol{\tau}=2\eta D, \tag{6.6}$$

is given by

$$\tau=\begin{bmatrix}\dfrac{2\eta\alpha}{1-2\alpha\lambda}&0&0\\0&\dfrac{-\eta\alpha}{1+\alpha\lambda}&0\\0&0&\dfrac{-\eta\alpha}{1+\alpha\lambda}\end{bmatrix},\quad \alpha=\frac{2U\dot{s}}{l} \tag{6.7}$$

and the pressure function is given by

$$p-p_\infty = \tfrac{1}{2}\rho[U^2-|\nabla\phi|^2], \tag{6.8}$$

where

$$\phi(x,r) = \tfrac{1}{2}\alpha x^2-\alpha r^2 \tag{6.9}$$

is the velocity potential. This pressure function can be compared with the coefficient of δ_{ij} in (6.1). The two pressure functions are the same in steady extensional flow because $C+\hat{\beta}\phi_{,il}\phi_{,il}$ is a constant equal to $\frac{1}{2}\rho U^2$ at infinity. It follows then that

$$\sigma_{11} = -\tfrac{1}{2}\rho U^2+\frac{4\rho U^2\dot{s}^2}{2l^2}(x^2+\tfrac{1}{4}r^2)+\frac{4\eta\dot{s}U/l}{1-4\dot{s}\lambda U/l}. \tag{6.10}$$

After expanding the last term of (6.10) for small values of $4\dot{s}\lambda U/l$, we get

$$\sigma_{11} = -\tfrac{1}{2}\rho U^2+\frac{\rho U^2\dot{s}^2}{2l^2}(4x^2+r^2)+4\eta\frac{U}{l}\dot{s}+16\lambda\eta\left(\frac{U\dot{s}}{l}\right)^2+O\left\{\left(\frac{U\dot{s}}{l}\right)^3\right\} \tag{6.11}$$

If we truncate (6.11) at second order, we recover σ_{11} given by (6.5) for a second-order fluid with the quadratic constants expressed in terms of the model parameters of the UCM,

$$2\alpha_2-\alpha_1 = 8\lambda\eta. \tag{6.12}$$

A second feature of the sedimentation of flat edged cylinders and plates in viscoelastic liquids with $Re < 1$ and $M < 1$ which begs for explanation is the presence of a small tilt from the vertical which we have called shape tilting. We have already noted that shape tilting appears whenever the particle has a flat edge with a square corner and does not appear to any appreciable extent when the ends are cone shaped or round (cf. figures 4, 7 and 10–12). We have the idea that this tilt is an effect of normal stresses and in particular of extensional stresses with reversed sign. The pulls of the reversed extensional stresses at stagnation points to align the cylinder axis with the stream as is suggested by figure 1, but the stagnation points move as the cylinder turns and they move to the first sharp corner they encounter. You can understand this by studying figure 1 with tension at the points s. Of course, the fore and aft symmetry of potential flow will not hold in the real flow and are not essential to this line of thought.

Carrying the idea of the previous paragraph a little further, we note that the absence of a flat end on the cylinders with round and cone shaped ends means the stagnation point can move to the far end of the cylinder, pulling it into good alignment with the stream. This is observed. Leal & Zana in Leal (1975) dropped a cylinder with one cone and one round end (length 0.681 inches and maximum diameter 0.053 in.) in a Separan AP-30 solution and they found that the point-down orientation was only marginally stable and the particle preferred the point-up. This suggests a strong pull at the pointed end which is consistent with the mechanism we have suggested and wake observations of Hassager (1979), and of Armour, Muirhead & Metzner (1984).

Shape tilt is important since it is a sensitive indicator of rheological properties of the fluid. Moreover the tilt properties of different shaped particles can be a starting place for the control of microstructure in particle-laden viscoelastic liquids.

Inertial tilting with $Re > 1$ and $M > 1$ has been discussed at the end of §5. We again note that arguments given there do not apply to Newtonian liquids or to weakly non-Newtonian liquids. We are uncertain about the criteria we ought to apply to distinguish non-Newtonian from Newtonian liquids. Joseph (1990) argued that the effective Newtonian viscosity μ in the Oldroyd B model,

$$\lambda\overset{\Delta}{\boldsymbol{\tau}}+\boldsymbol{\tau} = 2\eta\boldsymbol{D}[\boldsymbol{u}]+2\mu\lambda\overset{\Delta}{\boldsymbol{D}}, \tag{6.13}$$

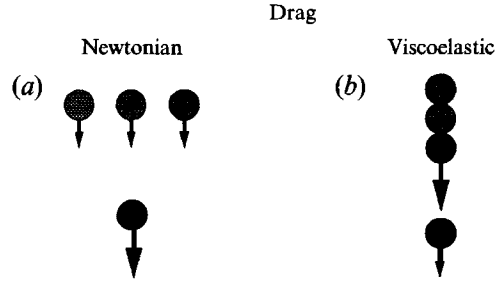

FIGURE 14. Drag on many spheres and a single sphere in Newtonian and viscoelastic liquids. (*a*) A single particle falls faster than the cross-stream array. The drag on many is greater than the drag on one. (*b*) A single particle falls slower than a chain of spheres. The drag on many is less than the drag on one.

is relatively small in liquids that are effectively viscoelastic, with well-defined wave speeds $c = (\eta/\lambda\rho)^{\frac{1}{2}}$. The effective Newtonian viscosity arises from the decay of fast modes.

If $\mu = 0$, then (6.13) is a Maxwell model, and if μ/η is small, then (6.13) is a perturbed Maxwell model, with Δ representing an 'invariant' derivative, say a covariant derivative. The normal stresses are embedded in the nonlinear terms defining this derivative, so that if λ is large, the normal stresses are large.

If the ratio μ/η of the Newtonian to the elastic viscosity is close to one the liquid is a perturbed Newtonian liquid with a small elastic viscosity. These fluids will respond like Newtonian liquids with inertia effects controlling orientation even when the ratio *Re* of inertia to viscous forces is surpassingly small.

The existence of a window of Mach numbers near one in which the tilt angle transition takes place reminds us of delayed die swell (Joseph, Matta & Chen 1987; J1990 chapter 13; Joseph & Christodoulou 1993). In that problem the delay was initiated only at supercritical Mach numbers and the swell was gradual. In the fully swelled region the Mach number was always subcritical $M < 1$. It follows that there is always a point in the region in which the swelling is not complete where $M = 1$. The Mach number in this region is changing locally from $M > 1$ to $M < 1$. This swelled region then frames a window of Mach numbers. In the problem of delayed die well hyperbolic transitions were observed in all of 23 very different polymer liquids tested. In these experiments it was argued that the smoothing of the delayed swell in some of the liquids could be attributed to the action of an effective Newtonian viscosity.

The natural orientation of long sedimenting bodies is the key to understanding the flow induced microstructures which develop in the sedimentation of spheres (see Joseph *et al.* 1992*b*). When inertia controls the orientation of a long body, the body will puts its broadside perpendicular to the fall. The drag on the long body falling with its broadside perpendicular to fall is greater than if it falls with its broadside parallel to the fall. But the small drag configuration, parallel to the fall, is unstable. Spherical bodies in the same fluid will interact in such a way as to produce kissing spheres parallel to the stream, which are momentarily long bodies parallel to the stream. The instability of this orientation causes the spheres to tumble favouring arrangements of spheres in which the line of centres is across the stream. These cross-stream arrangements have a greater drag than a single sphere falling alone (see figure 14).

The sedimentation of spherical particles with $Re < 1$ and $M < 1$ is very remarkable. The spheres actually form long particles which settle as cylinders with their line of centres parallel to the flow; they form chains of spheres. The stable configuration for

these chains is parallel to the stream when $Re < 1$ and $M < 1$ but the chains tilt and then fall into cross-stream arrangements in the inertially dominated regime with $Re > 1$ and $M > 1$. The chained spheres experience much smaller drag than a single sphere (see figure 14).

An especially interesting feature of chaining spheres is associated with the forces that produce aggregation rather than dispersion. We are preparing a report about this. For now, it will suffice to note that when two spheres fall slowly in close proximity they tend to clump together if the distance between them is smaller than a certain critical value which depends on the orientation of the line between the centres. It is by no means necessary that the spheres be of the same size; even a plane wall will attract a sphere if the distance between them is initially small enough.

7. Conclusions

1. It is well known that a cylinder or flat plate settling in a viscous liquid will turn its broadside to the stream. The same body settling slowly in a viscoelastic fluid will turn its broadside parallel to the fall but a heavier body of the same shape which falls faster will again turn its broadside perpendicular to the fall.

2. There is a regime in which viscoelastic stresses, viscous stresses and inertia compete. This competition evidently decides the tilt angle which the broadside of a cylinder or flat plate makes with the direction of fall in steady flow. No matter how the body is oriented initially, it will eventually fall with a unique angle of tilt.

3. A tilted particle experiences a side force.

4. The tilt angle can be controlled by changing the concentration of the solution using the same long body, cylinder or flat plate, or by changing the weight of the body in the same solution. In concentrated solutions the body settles straight-down. In dilute solutions it settles broadside-on.

5. The shape of the ends of the cylinder has an effect on the tilt angle, with rounded ends giving a larger angle of tilt (from the horizontal), as in the viscoelastic case. Squared off cylinders with flat ends tilt away from the vertical more than smooth ends in situations where cylinders with smooth ends settle straight-down. Tilting due to shape may be due to large normal extensional stresses at the corners. Shape tilting has a different origin than inertial tilting.

6. Rectangular flat plates which fall slowly with their broadside parallel to the flow, tilt one corner up in the plane in which they fall (figure 2).

7. A cylinder or flat plate falling in more dilute solutions have a higher terminal velocity which induces inertial effects and causes the body to turn broadside-on.

8. Increasing the temperature of a solution has the same effect on the tilt angle as decreasing the concentration.

9. Cylinders or flat plates centre themselves rigorously between the close walls of a sedimentation channel. The centring is very dramatic. The centreline of the cylinder and thin side of the plate are constrained to fall in the centreplane parallel to the walls of the channel.

10. The tilt angle transition appears to be a critical transition with straight-down sedimentation only when viscosity and viscoelasticity dominate ($Re < 1$, $M < 1$) and broadside-on sedimentation only when inertia dominates ($Re > 1$, $M > 1$). In viscous fluids inertia will eventually turn long particles broadside-on, no matter how small $Re > 0$ may be. Relatively larger ratios $Re > 1$ of inertial to viscous forces are required to turn long particles stabilized in straight-down orientations by viscoelastic forces.

11. The viscoelastic Mach number $M = U/c$ can be interpreted as a ratio of an

elastic length λU upon a viscous length ν/U. The condition $M > 1$ was satisfied in each and every realization of broadside-on settling, without exception, when c was the value measured on the wave speed meter.

The qualitative properties of tilting cylinders, plate and other bodies with a broadside are robust features which apply to all the viscoelastic fluids we have encountered: polymer solutions, amorphous polymers and many commercial shampoos. We are investigating the idea that the orientation of long bodies in a stream is the key to understanding the flow-induced microstructures which appear when swarms of spheres are placed in the same stream.

This paper is dedicated to the memory of Joe Matta.

Our work was supported by the NSF, fluid, particulate and hydraulic systems, by the US Army, Mathematics and AHPCRC, and by the DOE, Department of Basic Energy Sciences. We wish to thank R. Bai for his help with experiments and video tape recording, G. Ribeiro for suggesting that we plot the tilt angle against $Re\,W$ and for other comments, and J. Zhang, T. Blomstrorm, M. Arney, S. Braasch and H. Vinagre who measured the rod climbing constants, shear wave speeds, shear viscosities and other rheological properties and interfacial tensions of tested liquids.

REFERENCES

AMBARI, A., DESLOUIS, C. & TRIBOLLET, B. 1984 Coil-stretch transition of macromolecules in laminar flow around a small cylinder. *Chem. Engng Commun.* **29**, 63–78.

ARMOUR, S. J., MUIRHEAD, J. C. & METZNER, A. B. 1984 Filament formation in viscoelastic fluids. In *Advances in Rheology. Vol. 2, Fluids* (ed. B. Mena, A. Garcia-Bejon & C. Rangel-Nafaile), pp. 143–151. Universidad Nacional Autónoma De México.

BEAVERS, G. S. & JOSEPH, D. D. 1975 The rotating rod viscometer. *J. Fluid Mech.* **69**, 475–511.

BRUNN, P. 1977 The slow motion of a rigid particle in a second-order fluid. *J. Fluid Mech.* **82**, 529–550.

CHIBA, K., SONG, K. & HORIKAWA, A. 1986 Motion of a slender body in quiescent polymer solutions. *Rheol. Acta* **25**, 380–388.

CHO, K., CHO, Y. I. & PARK, N. A. 1992 Hydrodynamics of a vertically falling thin cylinder in non-Newtonian fluids. *J. Non-Newtonian Fluid Mech.* **45**, 105–145.

COLEMAN, B. D. & NOLL, W. 1960 An approximation theorem for functionals, with applications in continuum mechanics. *Arch. Rat. Mech. Anal.* **6**, 355–370.

COX, R. G. 1965 The steady motion of a particle of arbitrary shape at small Reynolds numbers. *J. Fluid Mech.* **23**, 625–643.

CROCHET, M. J. & DELVAUX, V. 1990 Numerical simulation of inertial viscoelastic flow, with change of type. In *Nonlinear Evolution Equations that Change Type* (ed. B. Keyfitz & M. Shearer). IMA Vol. 27, pp. 47–66. Springer.

FRAENKEL, L. E. 1988 Some results for a linear, partly hyperbolic model of viscoelastic flow past a plate. In *Material Instabilities in Continuum Mechanics and Related Mathematical Problems* (ed. J. M. Ball), pp. 137–146. Clarendon.

FRAENKEL, L. E. 1991 Examples of supercritical, linearized, viscoelastic flow past a plate. *J. Non-Newtonian Fluid Mech.* **38**, 137–157.

GOLDSHTIK, M. A., ZAMETALIN, V. V. & SHTERN, V. N. 1982 Simplified theory of the near-wall turbulent layer of Newtonian and drag-reducing fluids. *J. Fluid Mech.* **119**, 423–441.

HASSAGER, O. 1979 Negative wake behind bubbles in non-Newtonian liquids. *Nature* **279**, 402–403.

HERMES, R. A. & FREDRICKSON, A. G. 1967 Flow of viscoelastic fluids past a flat plate. *AIChE J.* **13**, 253–259.

HIGHGATE, D. J. 1966 Particle migration in cone-plate viscometry of suspensions. *Nature* **211**, 1390–1391; and in *Polymer Systems: Deformation and Flow* (ed. D. J. Highgate & R. W. Whorlow), pp. 251–261, 1968. Macmillan.

HIGHGATE, D. J. & WHORLOW, R. W. 1969 End effects and particle migration effects in concentric cylinder rheometry. *Rheol. Acta* **8**, 142–151.

HU, H. H. & JOSEPH, D. D. 1990 Numerical simulation of viscoelastic flow past a cylinder. *J. Non-Newtonian Fluid Mech.* **34**, 347–377.

JAMES, D. F. 1967 Laminar flow of dilute polymer solutions around circular cylinders. PhD thesis. Cal. Inst. Tech. Pasadena.

JAMES, D. F. & ACOSTA, A. J. 1970 The laminar flow of dilute polymer solutions around circular cylinders. *J. Fluid Mech.* **42**, 269–288.

JOSEPH, D. D. 1985 Hyperbolic phenomena in the flow of viscoelastic fluids. In *Viscoelasticity and Rheology* (ed. A. S. Lodge, J. Nohel & M. Renardy), pp. 235–321. Academic.

JOSEPH, D. D. 1990 *Fluid Dynamics of Viscoelastic Liquids*. Springer.

JOSEPH, D. D. 1992 Bernoulli equation and the competition of elastic and inertial pressures in the potential flow of a second order fluid. *J. Non-Newtonian Fluid Mech.* **42**, 385–389.

JOSEPH, D. D., ARNEY, M. S., GILLBERG, G., HU, H., HULTMAN, D., VERDIER, C. & VINAGRE, T. M. 1992*a* A spinning drop tensioextensiometer. *J. Rheol.* **36**, 621–662.

JOSEPH, D. D. & CHRISTODOULOU, C. 1993 Independent confirmation that delayed die swell in a hyperbolic transition. *J. Non-Newtonian Fluid Mech.* **48** (to appear).

JOSEPH, D. D. & LIAO, T. Y. 1993 Viscous and viscoelastic potential flow. In *Trends and Perspectives in Applied Mathematics, vol. 100, Applied Mathematical Sciences*. Springer.

JOSEPH, D. D., MATTA, J. & CHEN, K. 1987 Delayed die swell. *J. Non-Newtonian Fluid Mech.* **24**, 31–65.

JOSEPH, D. D., NARAIN, A. & RICCIUS, O. 1986*a* Shear-wave speeds and elastic moduli for different liquids. Part 1. Theory. *J. Fluid Mech.* **171**, 289–308.

JOSEPH, D. D., NELSON, J., HU, H. H. & LIU, Y. J. 1992*b* Competition between inertial pressures and normal stresses in the flow induced anisotropy of solid particles. In *Theoretical and Applied Rheology* (ed. P. Moldenaers & R. Keunings), pp. 60–65. Elsevier.

JOSEPH, D. D., RICCIUS, O. & ARNEY, M. S. 1986*b* Shear-wave speeds and elastic moduli for different liquids. Part 2. Experiments. *J. Fluid Mech.* **171**, 309–338.

LEAL, L. G. 1975 The slow motion of a slender rod-like particles in a second-order fluid. *J. Fluid Mech.* **69**, 305–337.

LEAL, L. G. 1980 Particle motions in a viscous fluid. *Ann. Rev. Fluid Mech.* **12**, 435–476.

LIU, Y. J. & JOSEPH, D. D. 1993 Sedimentation of particles in polymer solutions: experimental data. *AHPCRC preprint* 93-032.

MICHELE, J., PÄTZOLD, R. & DONIS, R. 1977 Alignment and aggregation effects in suspensions of sphere in non-Newtonian media. *Rheol. Acta* **16**, 317–321.

PETIT, L. & NOETINGER, B. 1988 Shear-induced structure in macroscopic dispersions. *Rheol. Acta* **27**, 437–441.

ROSCOE, R. 1965 The steady elongation of elasto-viscous liquids. *Brit. J. Appl. Phys.* **16**, 1567–1571.

THOMPSON, W. & TAIT, P. G. 1879 *Natural Philosophy* (2nd edn). Cambridge University Press.

ULTMAN, J. S. & DENN, M. M. 1970 Anomalous heat transfer and a wave phenomenon in dilute polymer solutions. *Trans. Soc. Rheol.* **14**, 307–317.